UNIVERSITY OF VAASA

FACULTY OF TECHNOLOGY

AUTOMATION TECHNOLOGY

Krista Rahunen

TESTING OF DISPLAYS OF PROTECTION AND CONTROL RELAYS WITH MACHINE VISION

Master's thesis for the degree of Master of Science in Technology submitted for inspection, Vaasa, 27th March, 2017.

Supervisor	Prof. Jarmo Alander
Instructor	Lic.Sc.Kimmo Kallio

FOREWORDS

This is my second Master's thesis, which I found to be as challenging as the first one. But at the same time, I can see a lot of improvement in the work flow and writing process. My previous studies have given me strong basis for the automation engineering and this thesis was natural choice to continue my career.

I would like to thank Kari Latva-Rasku, who introduced me to Kimmo Kallio. Much thanks to Kimmo and ABB, Medium Voltage Products, to giving me this opportunity. I am also grateful for Kimmo, Hannu Anttila and Petteri Vaara for all the help and support during this work. A huge thanks to the RTO employees for your help.

Further, I would like to thank Professor Jarmo Alander for your help and guidance during the thesis and these couple of years in the University of Vaasa.

Finally, I would like to thank my family and friends for all your support.

Vaasa, 27th March 2017
Krista Rahunen

TABLE OF CONTENTS

SYMBOLS AND ABBREVIATIONS

ABB	Asea Brown Boweri
3D	Three-Dimensional
CCD	Charge-Coupled Device
CMOS	Complementary Metal Oxide Semiconductor
DOF	Depth of Field/Depth of Focus
EMC	Electromagnetic Compatibility
f	focal length
FOV	Field of View
FPY	First Pass Yield
HMI	Human Machine Interface
IEC	International Electrotechnical Commission
IED	Intelligent Electronic Device
JND	Just-Noticeable Difference
LabVIEW	Laboratory Virtual Instrument Engineering Workbench
LCD	Liquid-Crystal Display
LED	Light-Emitting Diode
m	magnification
mm	millimetre
MVP	Medium Voltage Products
NCC	Normalized Cross Correlation
NI	National Instruments (company)

PCBA	Printed Circuit Board Assembly
ROI	Region of Interest
SAD	Sum of Absolute Differences
SCADA	Supervisory Control and Data Acquisition
SNR	Signal-to-Noise Ratio
SSD	Sum of Squared Differences
SSO	Spatial Standard Observer
TFT	Thin Film Transistor
UI	User Interface

UNIVERSITY OF VAASA
Faculty of technology
Author: Krista Rahunen
Topic of the Thesis: Testing of displays of protection and control relays with machine vision
Supervisor: Prof. Jarmo Alander
Instructor: Lic. Sc.Kimmo Kallio
Degree: Master of Science in Technology
Major of Subject: Automation Technology
Year of Entering the University: 2015
Year of Completing the Thesis: 2017 **Pages:100**

ABSTRACT

Human-machine interface is the link between a user and a device. In protection and control relays the local human machine interface consist of a display, buttons, light-emitted diode indicators and communication ports. Human-machine interfaces are tested before assembly with visual inspection to ensure quality of LCDs and LEDs. The visual inspection test system of HMIs consists of a camera and lens, a light emitted diode analyser, software and a computer. Machine vision operations, such as corner detection and template matching, are used to process and analyse captured images.

Original camera and measurement device set-up have been used several years, and it should be upgraded. New camera and lens were installed in the system, and the aim of the thesis was to evaluate and improve the testing set-up and software to support each other, to get better images, and further, to improve the first pass yield.

Camera position and settings were adjusted to capture images with good quality. Features of upgraded set-up and software were tested, and development ideas are given for further improvement. Changes in the set-up and software show promising results by giving more accurate test results from production.

KEYWORDS: machine vision, protection and control relay, LCD, image processing, testing, HMI

VAASAN YLIOPISTO
Teknillinen tiedekunta
Tekijä: Krista Rahunen
Diplomityön nimi: Suojareleiden näyttöjen testaus konenäön avulla
Valvojan nimi: Prof. Jarmo Alander
Ohjaajan nimi: Tk.L. Kimmo Kallio
Tutkinto: Diplomi-insinööri
Oppiaine: Automaatiotekniikka
Opintojen aloitusvuosi: 2015
Diplomityön valmistumisvuosi: 2017 **Sivumäärä:100**

TIIVISTELMÄ

Käyttöliittymä on työkalu ihmisen ja laitteen välillä, jolla saadaan tietoa laitteen toiminnasta, ja jolla käyttäjä voi ohjata laitteen toimintoja. Suojareleiden käyttöliittymä, toisin sanoen releen näyttö, sisältää nestekidenäytön, nappeja, valodiodi (LED) merkkivaloja ja kommunikaatioportin. Releiden näyttöä testataan visuaalisella tarkistuksella, jossa tulevat ilmi ongelmat nestekidenäytössä ja LED:ssä. Testisysteemi sisältää kamera, linssin, LED analysaattorin, testiohjelmiston ja tietokoneen. Otettuja kuvia analysoidaan konenäön keinoin. Operaatioihin kuuluvat kulmien havainnointi, mallikuvien käyttö vertailussa, kuolleiden pikseleiden havainnointi ja intensiteetin mittaus.

Testaussysteemiin vaihdettiin uusi kamera ja linssi, koska edelliset olivat olleet käytössä kauan. Työn tarkoituksena oli arvioida uusi laitteisto ja ohjelmisto, sekä niiden yhteensopivuus ja mahdollisuudet. Lisäksi, laitteisto täytyi säätää ja testata, jotta tuotteiden testausta voidaan parantaa. Tavoitteena oli saada parannettua tuotteiden läpimenoprosenttia, vanhalla laitteistolla mittauksissa esiintyy virheitä, jotka johtuvat testi laitteistosta tai -ohjelmistosta.

Kameran ja linssin paikkaa ja asetuksia muutettiin, jotta tulokseksi saatiin laadukas kuva. Laitteiston ja ohjelmiston ominaisuudet testattiin. Tämän jälkeen pohdittiin systeemin kehittämistä ja mahdollisia jatkotoimenpiteitä. Jo tässä työssä tehdyillä muutoksilla saatiin aikaan kehitystä LCD testauksessa.

AVAINSANAT: konenäkö, suojarele, nestekidenäyttö, kuvankäsittely, testaus, käyttöliittymä

1. INTRODUCTION

This Master's thesis studies testing of the displays of protection and control relays. The work was done at ABB Medium Voltage Product (MVP) located in Vaasa, Finland, for the Global Manufacturing Support -team that develops test devices and solves MVP production testing issues globally.

Liquid-crystal displays (LCDs) are widely used in electronic devices, such as televisions, mobile phones and laptops as a part of a human-machine interface (HMI). In industry, HMIs and LCDs are used to monitor and control devices, for example assembly lines or robots. The relay models used in this work are from the Relion® product family. The models have different types of HMIs, consisting of LCDs and light-emitting diodes (LEDs).

In ABB, at the department of MVP, the first pass yield (FPY) of HMI is notably lower than the FPY of any other module of the relay. Lower FPY means higher HMI module manufacturing costs, as modules need to be repaired and tested again. In most manufacturing industries – especially in mass-production - one goal is to achieve 100% quality assurance of the parts, subassemblies, and finished products. In generally, yield rate can be improved and costs can be reduced by installing the inspection devices in the design, layout, fabrication, assembly, and testing processes of production lines. (Huang and Pan 2015) Precisely designed testing systems and adapters can increase quality significantly, as quality control becomes automatic and further, consistent.

Product inspection is an important step in the manufacture process and the goal is to ensure that the quality of each product meets the standards. Inspection tasks are time consuming, and often performed by humans. The performance of the inspectors is imperfect, and the accuracy can vary because of the fatigue of the task. Human inspectors' skills require time to develop and workers have short working hours compared to machines, which affects the choices of manufacturers when they consider costs. (Huang and Pan 2015)

ABB MVP factories and Printed Circuit Board Assembly (PCBA) -suppliers use ABB testing platforms around the world to ensure the quality and uniformity of the products and testing procedures. An automatic inspection system with better sensing devices, automatic equipment, and a combination of computer technology, which includes properties such as pattern recognition, image processing, and artificial intelligence, can run in real time, and be consistent, robust, and reliable (Huang and Pan 2015). For example, many camera and mobile phone manufacturers use machine vision applications to detect functional faults in their products.

The first part of the thesis will review the relay product families, and vision system and machine vision features. This will include basic knowledge of relays and more details about different relay series. "Machine vision systems" section includes camera and lens features, limitations, and machine vision processes and applications. These are reviewed considering the system and devices used in the work. The second part contains the introduction of the testing system and test runs made to test and simulate the system. Lastly, discussion and suggested development ideas are presented.

1.1 Aim of the thesis

HMI of the relay is tested before assembly to detect operation failures. Remarkable number of HMIs will not pass the regular test due to different reasons: LEDs, display lights or displays dead pixels. These fails will cause retests of the HMIs. Retesting increases working hours when tens of HMIs are tested again in a day. Part of the fails are not real functionality problems of HMIs but issues in software or hardware. To develop the system to detect less false fails will decrease the costs and increase productivity. Annually, this will have a considerable effect on the testing time and production costs.

Aim of this thesis is to study the testing system and the testing software, and try to specify the machine vision properties and possibilities of the system. The software was partly from industrial machine vision software company. The goal was to get better understanding of the machine vision tasks, and clarify what happens in the software. The

operations and their configuration data should be reviewed and evaluated. Moreover, the purpose is to identify the main problems of the system and try to find solutions to solve the problems. By taking these actions, improvement of FPY may be reached.

The work was accepted in Automaatiopäivät22 seminar organized by Suomen Automaatioseura as an oral presentation. The title of the presentation is 'Testing of displays of protection and control relays with machine vision' (Rahunen 2017).

1.2 Related work

Various companies offer machine vision cameras and visual inspection systems for display inspection. We will review National Instruments (NI), Keyence, Optofidelity and Orbis system in later chapters of the thesis. In addition, other LCD inspection systems are available, for example from I.S.X. Corp. (I.S.X. Corp.), Takano (Takano Co.,Ltd. Image Processing group) Nica Technologies (Nica technologies Pte. Ltd.), and Radiant vision systems (Radiant vision systems).

Some LCD manufacturers are still using human inspectors in LCD visual inspection to detect dysfunctionalities (Hitachi Joei Tech. Co.; Logic technologies). Siemens as a relay manufacturer uses human inspectors in relay assembly (Siemens 2011). In assembly and production processes, an automatic visual inspection and machine vision applications are mainly used to shape and part recognition, and image classification (Fujitsu 2015; Siemens Simatic).

Machine vision cameras and applications have been used to detect defects in the surface of an LCD (Chao and Tsai 2007; Tsai and Lai 2008; Jiang, Wang and Liu 2007). Techniques such as moving average filters, diffusion models and basis image technique have been used. Moreover, LCDs have phenomena called mura, which is a distortion that causes the uneven patches of changes in luminance.

Mostly, camera has better resolution than the human eye. That is why, systems with more like the human eye are developed (Watson 2006; Park and Yoo 2009). Watson (2006) has developed a spatial standard observer (SSO) which models human visual sensitivity to spatial patterns. It simplifies the human visual model and can measure the visibility of foveal spatial patterns, or the discriminability of patterns. It gives output in specifically defined units of just-noticeable difference (JND), which is the difference in visibility between the test and reference images. (Watson 2006) In addition, Park and Yoo (2009) approximate human perception degree with JND by using the regression analysis.

2. PROTECTION AND CONTROL RELAYS

ABB has a wide variety of protection and control relays (ABB Distribution Protection and Control). Protection and control relays for distribution automation made by ABB are designed to comply with by the International Electrotechnical Commission (IEC) 61850 standard for communication and interoperability of substitution automation devices. In this work, the control relays from the Relion® product family, the series 615, 620 and 630 are discussed. The 615 and the 620 series are from a product family of relays which are designed to protection, control, measurement and supervision of utility substations and industrial switchgear and equipment (ABB 2015)(ABB 2016). The 630 series is developed for protection, control, measurement and supervision of utility and industrial distribution substations, medium and large asynchronous motors in industrial power systems, and transformers in utility and industry power distribution networks. The 630 relays have seamless connectivity to various station automation, and supervisory control and data acquisition (SCADA) systems due to the IEC standards (ABB 2014).

These products comply with the directive of the Council of the European Communities on the approximation of the laws of the Member State relating to electromagnetic compatibility (EMC) (the EMC Directive 2004/108/EC), and concerning electrical equipment for use within specified voltage limits (the Low-voltage directive 2006/95/EC). Furthermore, conformity of the products results from tests conducted by ABB in accordance with the product standard EN 60255-26 for the EMC directive, and with the product standards EN 60255-1 and EN 60255-27 for the low voltage directive for the 615 series and the 620 series (ABB 2015)(ABB 2016), and EN 50263 and EN 60255-26 for the EMC directive, and with the product standards EN 60255-1 and EN 60255-27 for the low voltage directive for the 630 series (ABB 2014). Also, all the products are designed according with the international standards of the IEC 60255 series. (ABB 2014)(ABB 2015)(ABB 2016)

2.1 Human machine interface

HMI, or local HMI, is the link between the user and the device. In the protection and control relays, HMI is used for setting, monitoring and controlling the relay (ABB 2016). HMI consists of a LCD display, buttons, LED indicators and communication ports. Examples of HMIs are shown in Figure 1.

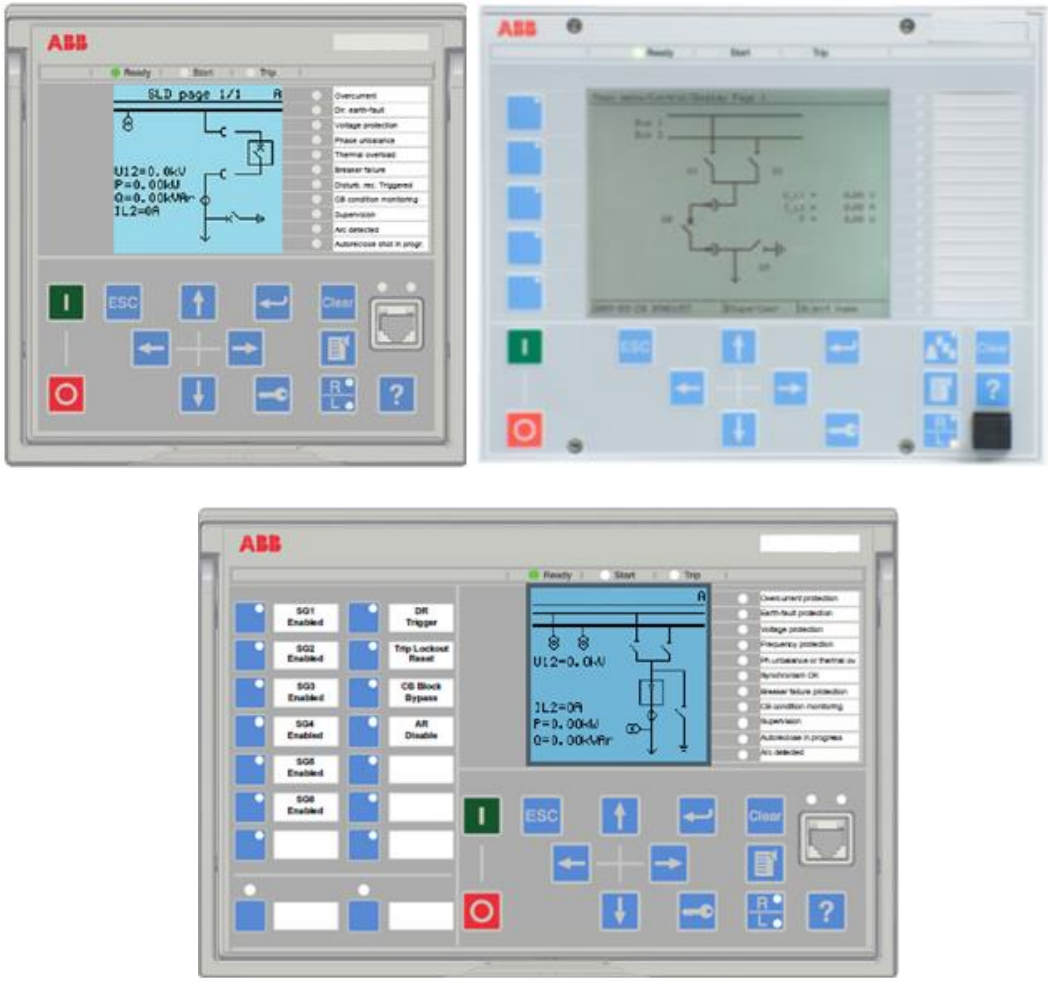

Figure 1. Examples of the local HMIs. Top left) 615 series, Top right) 630 series, Bottom) 620 series. The local HMI contains of LCD, LEDs and navigation buttons.

The HMI is a crucial part of giving information of the function of the relay. It shows errors and dysfunctionalities of the relay and the system where the relay is installed. The HMI gives information to the user who can make decisions and control the relay and the system. The LEDs show the status of the device. The HMI includes LCD panel, which is the main part of it. LCD can be used to give information for the user and user can control relay by using the LCD and buttons. The functions and using the HMI is reviewed more detailed in relay series chapter.

The Main menu covers main groups which are divided into more detailed submenus: control, events, measurements, disturbance records, settings, configuration, monitoring, tests, information, clear and language (ABB 2014)(ABB 2015)(ABB 2016) The examples of menu and single-line diagram from series 615 and 620 are shown in Figure 2, and from series 630 in Figure 3.

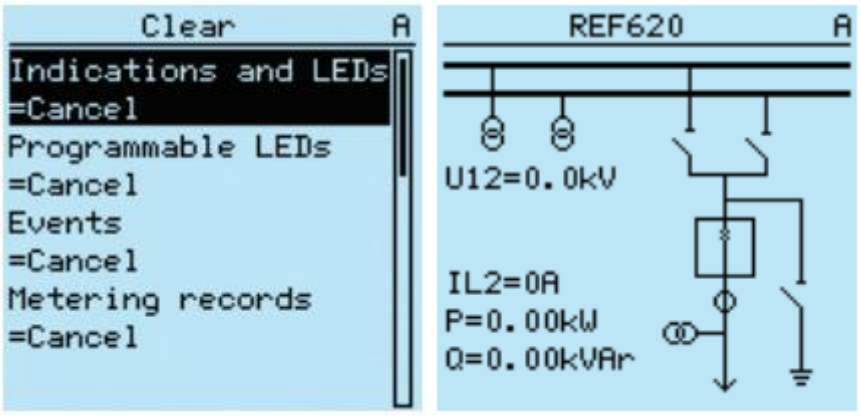

Figure 2. Examples from the view of the 615/620 series LCD display. Left) menu and scroll bar. Right) example of single-line diagram (ABB 2015)

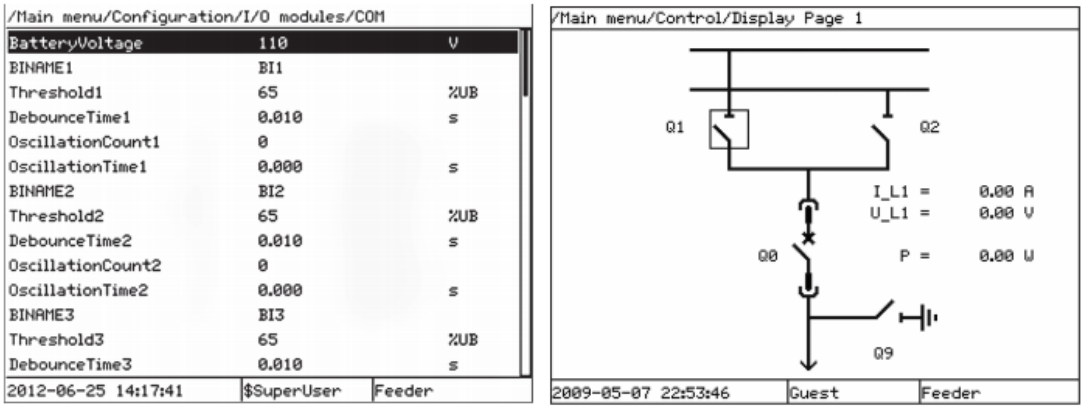

Figure 3. Examples from the view of the 630 series LCD display. Left) the menu and scroll bar. Right) example of single-line diagram (ABB 2014)

2.2 Relion 615, 620 and 630 series

In 615 series, the HMI includes a graphical liquid-crystal display (LCD), LEDs and buttons. The positions of the buttons, LCD and LEDs are shown in Figure 4. Three protection indicator LEDs are set above the display. They are Ready, Start and Trip. Moreover, there are 11 matrix programmable LEDs next to the display in front of the HMI. Push buttons are appointed in the keypad for navigating in different menus and views, to acknowledge alarms, reset indications, provide help, and switch between local and remote control mode. In addition, with the push buttons open and close commands can be given to objects in the primary circuit. (ABB 2016) Comparison to 620 and 630 series is shown in Table 1.

The 620 series uses the same type of large LCD as the 615 series. The HMI in the 620 series is bigger and contains a monochrome LCD, bush buttons with indicator LEDs, similar bush buttons and indicator LEDs as in 615 series. The difference is that the HMI keypad on the left side of the protection relay contains 16 programmable push buttons with red LEDs. The buttons and LEDs are freely programmable, and they can be configured both for operation and acknowledgement purposes. The LEDs can also be independently configured to bring general indications or important alarms to the

operator's attention. To provide a description of the button function, it is possible to insert a paper sheet behind the transparent film next to the button. (ABB 2015)

The 630 series HMI contains a graphical monochrome display with a resolution of 320×240 pixels. The display view is divided into four basic areas. The path shows the current location in the menu structure. If the path is too long to be shown, it is truncated from the beginning, and the truncation is indicated with three dots. (ABB 2014)

The HMI includes three protection-status LEDs above the display: Ready, Start and Trip. Furthermore, there are 15 programmable alarm LEDs on the front of the HMI. Each LED can indicate three states with the colors: green, yellow and red. Altogether, the 15 physical three-color LEDs can indicate 45 different alarms. The LEDs can be configured with PCM600. (ABB 2014)

The matrix programmable LEDs are for alarm indication and every colour indicates different status. These colours for every LED are individually controllable and can be either green or red. Red is alarm colour and green can indicate either normal status or normal operation. (ABB Engineering manual)

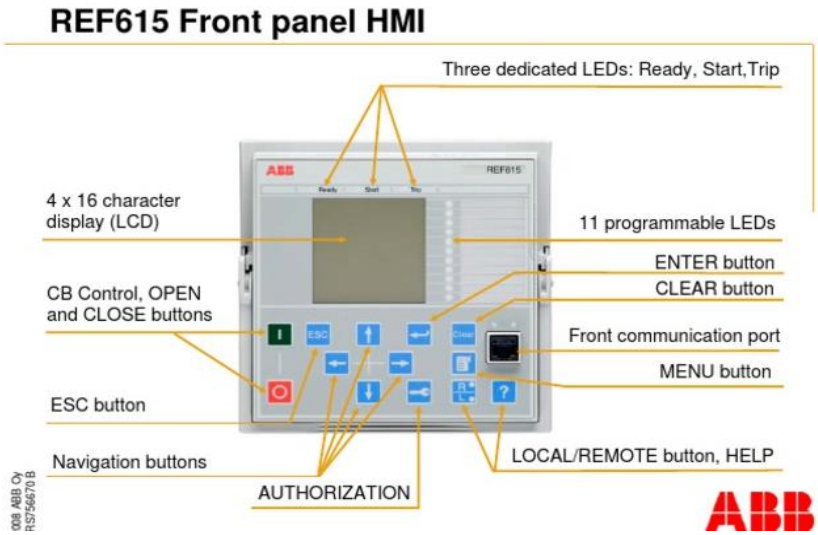

Figure 4. The buttons, display and LEDs of the local HMI. (ABB Database)

Table 1. Comparison of HMIs.

Model series	**615**	**620**	**630**
Programmable LEDs, colours • green • red • yellow	11 x x -	11 x x -	15 x x x
Indicator LEDs	3	3	
LCD resolution	128×128 65×128	128×128	320×240
Buttons	11/13	13	14
Programmable push buttons with LEDs	-	16, red	5
Character sizes	2	2	2

3. MACHINE VISION SYSTEMS

Machine vision has become useful in industry, as it has helped to automate visual tasks in industry. Machine vision can be determined to method and technology used, example in process control and robot guidance, to automate visual inspection and analysis. Machine vision systems are commonly used in industry in quality control tasks, such as defect detection, identifying parts, sorting, positioning, code scanning, and dimension measurements. (Sergiyenko and Rodriquez-Quinonez 2016).

Designing a machine vision system includes many aspects that are be considered before making or buying one. For example, desired optical properties depend on variations of targets, their movement and environment, triggering and chosen image processing methods will have an effect to the measurement time and accuracy. Also, user interface, integration to other systems, and hardware and software need to be thought. (Telljohann, 2006) For optimal system performance, optics should be chosen well. Next properties are most important: object-image distance, magnification (focal length), required depth of field, aperture, minimum relative illumination, maximum permissible distortion and mechanical interfaces, such as maximum diameter and length, maximum weight and interface to the camera (C-mount or D-mount) (Lenhardt 2006). In addition, in business world, costs and development time are in high value.

This chapter reviews vision systems by starting from human vision system, continuing to camera properties, and finally inspects machine vision and image processing methods. In the end of the chapter is comparison of various industrial machine vision software.

3.1 Human vision

The human vision system can be divided into two major components: the eyes and the visual pathways in the brain. The former capture light and convert it into signals that can be understood by the nervous system and the latter transmits and process those signals.

Multiple phenomena of visual perception have relevance to digital imaging as from the optical point of view the eye can be thought of as a photographic camera. (Winkler 2013) The eye contains of a system of lenses and a variable aperture to focus images on the light-sensitive retina. All optics in the eye follow the physical principles of refraction, where light rays bend between two transparent media that have different refractive indicates. Lenses converge or diverge light depending on the lens shape: a concave lens bent light rays outward and a convex lens inward when light rays are passing through the lens. (Hecht 1987; Guyton and Hall 2010)

The distance of the object from the lens affect to distances where the lens is focused. Gaussian lens formula is describing this:

$$\frac{1}{a} + \frac{1}{b} = \frac{1}{f}, \qquad (1)$$

where a is the distance between the source and the lens, b is the distance from the lens to the image and f is the focal lenght of the lens. The focal length is a presentation of the optical power of the lens. It shows how much the lens is capable to bent light rays. (Hecht 1987)

The human visual system can be adapted to a huge range of light intensities. One of the main mechanism is pupillary aperture, which can be mechanically variated. The variation of the pupil diameter can be between 1.5 and 8mm. The lens of the human eye is curvatured and its optical power can be voluntarily increased by contracting muscles around it. This is called accommodation and it is way to bring objects at focus in different distances. (Guyton and Hall 2010)

Human eye sees light intensity differently compared to a camera. Hue can be defined to be human sensation of similarity of colour areas (red, yellow, green and blue). Saturation is the seen colourfulness with relation to a brightness, which is human sensation about

lightness over an area. With camera saturation is defined from 0 to 1 (or 255), to define a brightness of a colour plane. Then saturated image is seen as bright white.

3.2 Camera and optics

Camera manufacturers and camera properties need to be considered before choosing a camera, optics and a software. The camera manufacturer must be chosen to support the software used in the testing system. Furthermore, triggering, the size of the camera, user interface, parameter control, sensor, integration, and price are camera properties, which are thought. The main point of choosing a camera is the sensor in it. However, two cameras with a different manufacturer with the sensor by third manufacturer may have very different performance and properties. The differences are caused by the design of the interface electronics. (Edmund optics 2011) By choosing the sensor, also pixel and resolution properties will be chosen. Moreover, the frame rate and shutter speed are properties, which are determined by the sensor.

Two different kind of sensors are widely used in machine vision systems: a metal–oxide–semiconductor (CMOS) and charge-coupled device (CCD) sensor. CMOS sensors have lower energy consumption and smaller camera size. The CMOS sensor has lower signal-to-noise ratio (SNR), which means more noise and lower overall image quality, compared to the CCD sensor. (Wang 2008) Images captured in the study include low contrast boundaries that can be lost due the noise and the CCD sensor with high dynamic range and uniformity will produce usable image quality. The CMOS sensor has is widely used in mobile phone cameras due to its small size. Also, use of CMOS sensors has been increasing in machine vision cameras. (Yole 2015)

A sensor frame rate should meet testing system requirements. The image rate should be slightly higher than what is the real image rate (Ahearn 2016). This means that if an image is taken 5 times in a second, the sensor should be able to take images more often and should have the frame rate equal to higher than 8-10fps.

3.2.1 Field of view

Field of view (FOV) gives the size of an object that can be imaged with the chosen sensor and magnification. Figure 5. shows the thin lens equation (1), which can be used to calculate focal length and magnification. These features are needed when choosing a camera and a sensor, and the calculation can be used to determine the camera distance from the target and the focal length, which measure how strongly the system converges or diverges light. (Hecht 1987)

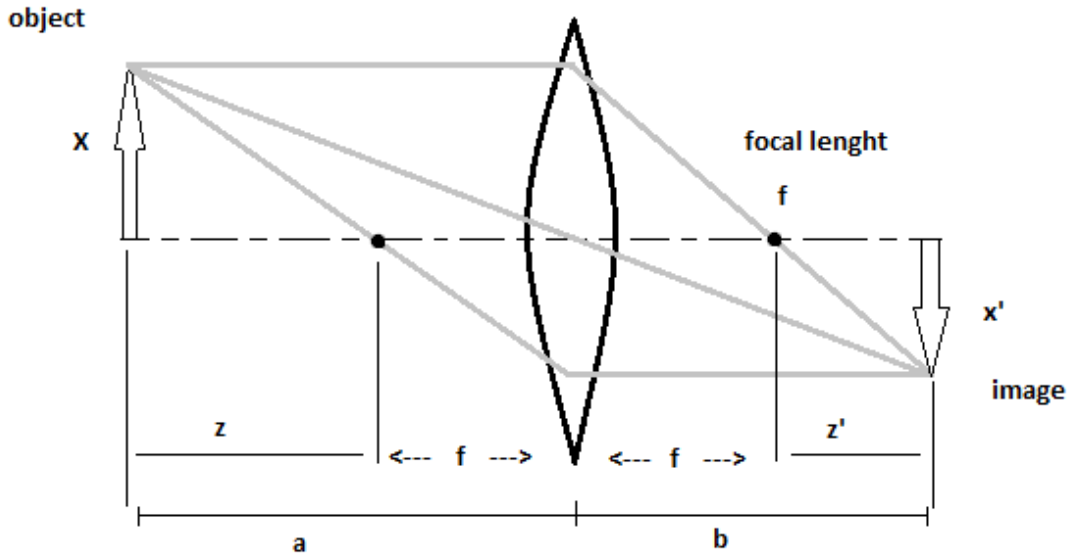

Figure 5. Thin lens equation. a is the distance of the object from the centre of the lens and b is the distance of the image from the centre of the lens, X and x' are the object and image heights respectively and f is the focal length.

We assume that $a = z + f$, and $b = z' + f$, then (2) can be written as

$$\frac{1}{z+f} + \frac{1}{z'+f} = \frac{1}{f}, \qquad (2)$$

which is used in the following calculations.

The magnification m of a lens system is defined

$$m = \frac{x'}{x} = \frac{b}{a} = \frac{z\prime+f}{z+f}, \quad (3)$$

and when $z \gg f$, then $z' \ll f$, and

$$m \approx \frac{f}{z} = \frac{z'}{f}. \quad (4)$$

This shows that the change of magnification can occur both from a change of the distance to the object and from a change of the focal length.

Finally, we can write an equation for the FOV that is

$$m = \frac{x'}{x} = \frac{D}{FOV} \quad (5)$$

$$\leftrightarrow FOV = \frac{D}{m}, \quad (6)$$

where D is the width of the image sensor. Here we can see that the FOV depends on the distance of the object, the image sensor size and the focal length. (Hecht 1987)

Many optical imaging systems include a variable aperture, which give them an ability to adapt to different light levels. Aperture means "opening", and describes the size of the hole in a lens, which the light passes through on its way to the camera's sensor. The aperture stop is an important element in most optical designs. Its most obvious feature is that it limits the amount of light that can reach the image plane. The aperture stop defines the size of the aperture, which depends of the use. If lot of light is needed, the aperture size should be big and when wanted to avoid saturation, aperture size is smaller. Aperture size is proportional to the focal length as the aperture is presented by f-number, which is focal length divided by diameter (Figure 6). (Hecht 1987; Jan Kamp 2013)

Size of the aperture affects to an occurrence of aberrations; too large aperture will cause distortions. Large aperture sizes cause also vignetting, which causes light fading near image pheriphery. Also, aperture have side effect, diffraction, which is scattering of the light and the phenomena will cause a blurred image. (Hecht 1987; Jan Kamp 2013)

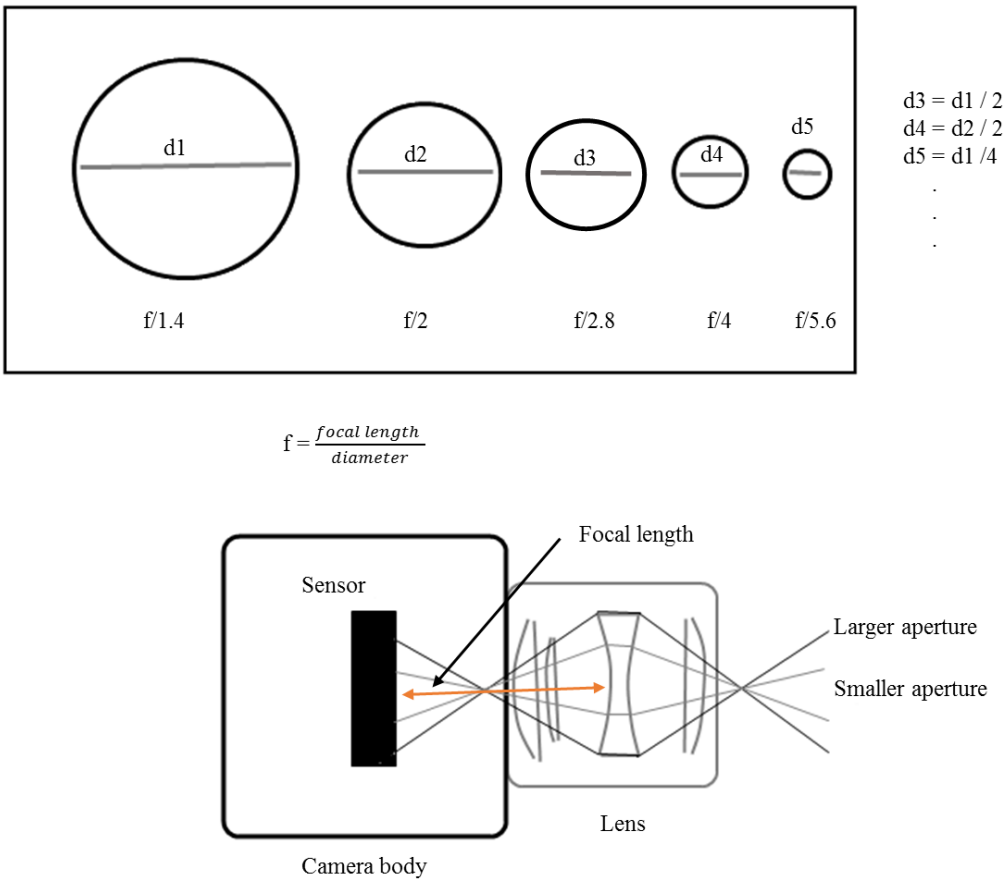

Figure 6. Comparison of aperture numbers. Top) comparison of the size of the aperture, where f is f-number and d illustrates a diameter of a circle. Aperture is proportional to the focal length as the f number is focal length/diameter. Bottom) Focal length and aperture size illustration by light rays.

3.2.2 Depth of focus and depth of field

In optics, particularly as it relates to film and photography, depth of field (DOF), also called focus range or effective focus range, is the distance between the nearest and farthest objects in a scene that appear acceptably sharp in an image, in other words the range of field where objects will appear in focus on the image plane (Figure 7.). Although a lens can precisely focus at only one distance at a time, the decrease in sharpness is gradual on each side of the focused distance, so that within the DOF, the unsharpness is imperceptible under normal viewing conditions. Aperture size (light level) will influence DOF: a large aperture produces images with small DOF and a small aperture produces images with large DOF. (Hecht 1987; Jan Kamp 2013)

The depth of focus and the depth of field are measurements that show how much the object can differ from the focus point before the quality of the captured image is in unacceptable level. When depth of field is the focus range, depth of focus can be related to blurring: the object outside the depth of focus will produce blurred image. The acceptable measures depend on features such as nature of the target and image detection methods. (Goodman 2010, Hecht 1987)

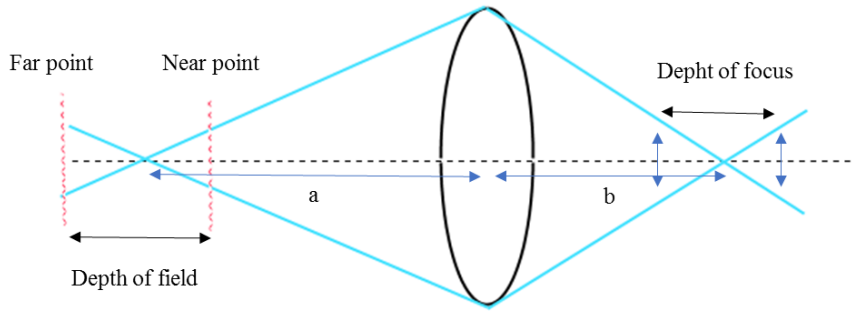

Figure 7. Depth of field and depth of focus. a is a lens distance from a target and b is a lens distance from an image plane.

3.2.3 Resolution

Resolution has many definitions depending on the source but it is always related to sharpness of the image. ISO 12233:2014 standard defines the resolution as "an objective analytical measure of a digital capture device's ability to maintain the optical contrast of modulation of increasingly finer spaced details in scene." (ISO 12233 2014) Furthermore, this is separated from the sharpness, which is more of an impression of details and edges of the image, not the feature of the camera nor sensor.

The final resolution of the image is due to the properties of the components of the camera system: camera module, sensor and image processing pipeline. The lens system and sensor can have different resolution and the former may have smaller resolution than the latter. Moreover, aberrations of the lens system decrease total resolution. (ISO 12233:2014) The image-processing pipeline often includes algorithms that affect the final resolution. Filtering algorithms, such as demosaicing, denoising and compression, may filter out the smallest details. However, algorithms can increase the subjective sharpness, for instance unsharp masking. (Peltoketo 2016)

3.3 Image quality, noise and lens artefacts

Image quality depends on many factors, such as camera properties and optics, lightning, the target and its distance. All these variables may be influenced by the user, and often, the image might still be degraded during capture, transmission or processing. For example, random errors degraded to an image are called noise and may occur during image capture, transmission or processing, and may be independent or dependent on image content. Usually, noise is described by its statistical characteristic, for example white noise or its special case, Gaussian noise. (Steger 2006) The noise may need to be suppressed by using the image smoothing algorithms such as image averaging (Nagao and Matsuyama 1980), mean filtering (Steger 2006), median filtering (Tyan 1989) and Gaussian filtering (Lindeberg 1994).

Limitations in manufacturing of camera sensors and lenses cause issues in image processing and image quality. (Peltoketo, 2016) These limitations cause compromises when considering image processing algorithms and image quality needed, which depends on the target and the use of the image. For example, images with small details require higher image quality, in other words sharpness and low noise level. Sharpness is defined e.g. according to ISO 12233:2014 standard and Imatest Sharpness definition. The former defines sharpness with Spatial frequency response (SFR), which is a multi-valued metric that measures a contrast loss as a function of spatial frequency (ISO 12233 2014) and the latter defines sharpness as a determinant of "the amount of details an imaging system can reproduce" (Imatest Sharpness).

Keelan (2002) introduces four groups of attributes for the clarification of image quality. Those are artificial, prefential, aesthetic and personal attributes. The first group includes factors such as unsharpness and digital artefacts, the second group includes colour balance and contrast, the third group includes composition and the last one includes factors like how a person remembers certain cherished event. These can be measured objectively but for example can include perceptual components, such as color saturation. The Image quality, when inspected by human, is very personal and depend on perceptual attributes. (Keelan 2002)

When we want a lens to meet the requirements of machine vision application, the lens must be chosen to accurately reproduce the imaged object. This means that machine vision lenses must be as free as possible from any possible image distortion effects. Certainly, this depends on used application and needs. By understanding these effects and how they can be evaluated, the types of lenses can be chosen better to meet the needs of the application. (Wilson 2013)

Five types of lens aberrations are spherical aberration, coma, astigmatism, field curvature and distortion. Although, these five aberrations occur when monochromatic light passes through a lens. Furthermore, axial and lateral chromatic aberration may occur when polychromatic light is used. Any lens has some aberrations, but manufacturers try to minimize these effects. (Wilson 2013)

A distortion is defined to be a difference in a geometrical similarity between the object and the image. There are different types of distortion: pincushion, barrel and moustache distortion (Figure 8). In pincushion distortion, the magnitude of the magnification increases monotonically with field height and the image is stretched radially. In barrel distortion, the magnitude decreases, so the image is squeezed. The aberration coefficients can be positive or negative, as it follows power series, and the direction of distortion can change as a function of field height. Furthermore, the error is radial for rotationally symmetric lenses when object and image plane are perpendicularly located to the axis. (Goodman 2010, Hecht 1987)

Aperture size affect lens aberrations: if the size of the aperture is changed, the bordering ray (passes through in borders of the aperture), is changed, but the chief ray (passes through in the middle of the aperture) stay constant (Hecht 1978). Furthermore, if the aperture is reduced, depth of focus and depth of field increase and illumination of the image decreases. The images whit smaller aperture can be corrected better as the rays from axial object points are more nearly paraxial. (Goodman 2010, Hecht 1987)

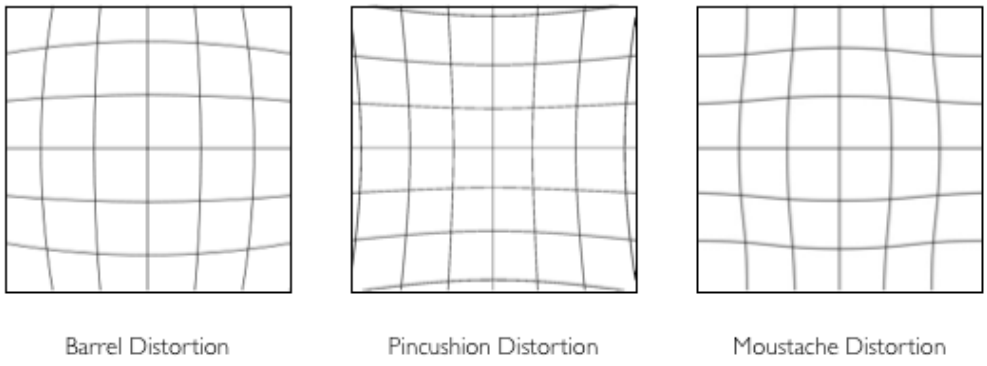

Figure 8. The lens distortions: barrel, pincushion, and moustache distortion. (Jan Kamp 2013)

3.3.1 Mean filtering

Noise can be reduced by averaging multiple images. Although the averaging process gives a very good estimation for the grey values, the method is not very fast and therefore other methods are mainly used in industrial applications. Ideally, only one image is enough to estimate the true grey values and noise. Temporal averaging can be replaced with a spatial averaging which is also known as mean filtering. It can be computed over a window of $(2n+1)\times(2m+1)$ pixels, called the mask and is written as follows:

$$g_{r,c} = \frac{1}{(2n+1)(2m+1)} \sum_{i=-n}^{n} \sum_{j=-m}^{m} \hat{g}_{r-i,c-j}. \quad (7)$$

In this method, the noise variance is reduced by a factor that corresponds to the square root of the number of measurements that are used to calculate the average. The problem of the method is that it blurs the edges. (Steger 2006)

3.3.2 Median and Nth order filtering

Median filter is a nonlinear filter, which can be used to reduce impulse noise, called salt and pepper type noise, and the blurring of edges. The idea of the filter is to replace the current point in the image by the median of the brightness's in its neighbourhood. The median is defined so that half of the values are larger than median and the other half of the values are smaller. The median value can be found by ordering the values and selecting the middle one. (Huang, Yang and Tang 1979; Tyan 1989) The median filter can be written as

$$g_{r,c} = \underset{(i,j)\in W}{\text{median}}\, \hat{g}_{r-i,c-j}. \quad (8)$$

Individual noise spikes do not influence the median brightness's of the neighbourhood, thus the median filter eliminates impulse noise well and it does not blur edges much. (Sonka et al. 2008) Median smoothing is a special case of rank filtering, where instead of choosing a median value, the other variant can be chosen. It can be, for example the

minimum or the maximum value. This leads to rank operations which can be thought as same as morphological operations. (Huang et al. 1979; Tyan 1989)

3.3.3 Spatial calibration

Spatial calibration is a method where computational pixel is transformed to real-world units. The transformation is important when accurate measurements in real-world units are required. In addition, spatial calibration can correct lens aberrations, which are artefacts caused by lens when light goes through the lens. A grid image, for example, dot image or chequered image, is used to determine a calibration information. Dots or squares are data points that have known measurements, such as distance between two points. In chequered image, straight lines have more comparison points than dots in dot image. Measurements in captured image are scaled to respond original measurements, in which case captured image is calibrated and distortions reduced.

3.4 Image processing methods for pattern recognition

In this chapter, different image processing methods are discussed. Focus is in methods that could be used in the HMI testing system of protection and control relays. LabVIEW is used to implement image processing algorithms. Labview offers image processing blocks and IMAQ toolboxes, which are for machine vision and image processing applications. Filters can be used to improve the image quality, sharpening and transforming the image. IMAQ Vision toolboxes comes with many filters, such as Gaussian filter for smoothing images, Laplacian filters for highlighting image details, Median and Nth order filters to noise removal, and Prewitt, Roberts and Sobel filters for edge detection. Furthermore, user defines filter coefficients. (National instruments 2010) Image processing methods include machine vision operations, such as template matching, corner detection, edge detection and morphological operations. All of these are some types of filters.

3.4.1 Template matching

Template matching is a technique to recognise patterns in images by using template images. The similarities between a source image and the template image are searched. The problem is to find the best match between these two with minimum distortion or maximum correlation. Most used similarity measures are the sum of absolute differences (SAD), the sum of squared differences (SSD), and the normalized cross correlation (NCC) (Wei and Lai 2008). Here are the formulas for the SAD and the NCC similarity measurements:

$$SAD(x,y) = \sum_{i=1}^{M}\sum_{j=1}^{N} |T(i,j) - I(x+i, y+j)| \,, \quad (9)$$

$$NCC(x,y) = \frac{\sum_{i=1}^{M}\sum_{j=1}^{N} I(x+i,y+j)\cdot T(i,j)}{\sqrt{\sum_{i=1}^{M}\sum_{j=1}^{N} I(x+i,y+j)^2}\cdot\sqrt{\sum_{i=1}^{M}\sum_{j=1}^{N} T(i,j)^2}} \,. \quad (10)$$

3.4.2 Edge detection

Edge detection is often used method in machine vision applications. Majority of the image processing and machine vision applications require some level edge detection, such as edge-based obstacle detection or edge-based target recognition. The idea of edge detection is to locate edges by identifying sharp discontinuities, in other words large pixel intensity differences, which form the boundaries (edges) in an image. False edge detection, noise and low contrast boundaries cause problems in edge detection. (Bhardwaj and Mittal 2012)

The problems can be reduced by image processing operators, which can be divided into two groups: the first order derivative and the second order derivative operations. The former uses thresholding to detect edges, and the latter uses extraction of zero-crossing points to find the maxima, which is used to locate boundaries. Roberts, Sobel and Prewitt edge detectors are in the first group and Laplacian of Gaussian, Canny edge detector,

basic declivity and modified declivity are included in second group of operators. Bhardwaj and Mittal's study shows that the declivity operators, which are operation that classify high amplitude declivities as edges, find more true edges compared to other edge detection methods. In case where first order derivative methods are too sensitive to noise distraction, Canny can be used to obtain better results. (Bhardwaj and Mittal 2012)

For image processing, Labview offers IMAQ tool that are shown in Table 2. (National instruments 2011). The edge detection block uses first derivative edge detectors, and the "IMAQ CannyEdgeDetection" uses canny edge detector. These techniques are introduced next.

Table 2. Labview IMAQ image processing tools.

Palette Object	**Description**
IMAQ GetKernel	Reads a predefined kernel.
IMAQ BuildKernel	Constructs a convolution matrix by converting a string. This string can represent either integers or floating-point values.
IMAQ Convolute	Filters an image using a linear filter. The calculations are performed with either integers or floating points, depending on the image type and the contents of the kernel.
IMAQ Correlate	Computes the normalized cross correlation between the source image and the template image.
IMAQ LowPass	Calculates the inter-pixel variation between the pixel being processed and those pixels surrounding it. If the pixel being processed has a variation greater than a specified percentage, it is set to the average pixel value as calculated from the neighbouring pixels.
IMAQ NthOrder	Orders, or classifies, the pixel values surrounding the pixel being processed. The data is placed into an array and the pixel being processed is set to the nth pixel value, the nth pixel being the ordered number.
IMAQ EdgeDetection	Extracts the contours (detects edges) in gray-level values.
IMAQ CannyEdgeDetection	Uses a specialized edge detection method to accurately estimate the location of edges even under conditions of poor signal-to-noise ratios.

In edge detectors, the gradient is used to approximate the local changes in an image. The gradient is a measure of change in a function when an image is considered to be an array

of samples of continuous function of image intensity. A discrete approximation of the gradient can be used to detect significant changes in grey values in an image. The gradient can be defined as the vector

$$G[f(x,y)] = \begin{bmatrix} G_x \\ G_y \end{bmatrix} = \begin{bmatrix} \frac{\partial f}{\partial x} \\ \frac{\partial f}{\partial y} \end{bmatrix}, \quad (11)$$

and for digital images, the approximation can be written as

$$G_x \cong f[i, j+1] - f[i,j] \quad (12)$$

$$G_y \cong f[i,j] - f[i+1, j]. \quad (13)$$

Roberts operator provides a simple approximation to the gradient magnitude

$$G\big[f[i,j]\big] = |f[i,j] - f[i+1, j+1]| + |f[i+1, j] - f[i, j+1]|, \quad (14)$$

and with using convolution mask

$$G\big[f[i,j]\big] = |G_x| + \big|G_y\big|, \quad (15)$$

where $G_x = \begin{bmatrix} 1 & 0 \\ 0 & -1 \end{bmatrix}$, and $G_y = \begin{bmatrix} 0 & -1 \\ 1 & 0 \end{bmatrix}$.

The Sobel operator is one of the most commonly used edge detectors and it is used to avoid having the gradient calculated about an interpolated point between pixels. It is the magnitude of the gradient M

$$M = \sqrt{s_x^2 + s_y^2}, \quad (16)$$

where $c = 2$, and

$$s_x = (a_2 + ca_3 + a_4) - (a_0 + ca_7 + a_6) \quad (17)$$

$$s_y = (a_0 + ca_1 + a_2) - (a_6 + ca_5 + a_4). \quad (18)$$

They can be implemented using convolution masks:

$s_x = \begin{bmatrix} -1 & 0 & 1 \\ -2 & 0 & 2 \\ -1 & 0 & 1 \end{bmatrix}$ and $s_y = \begin{bmatrix} 1 & 2 & 1 \\ 0 & 0 & 0 \\ -1 & -2 & -1 \end{bmatrix}$.

Same equations are used in Prewitt operator, except the constant $c = 1$:

$s_x = \begin{bmatrix} -1 & 0 & 1 \\ -1 & 0 & 1 \\ -1 & 0 & 1 \end{bmatrix}$ and $s_y = \begin{bmatrix} 1 & 1 & 1 \\ 0 & 0 & 0 \\ -1 & -1 & -1 \end{bmatrix}$.

(Jain, Kasturi and Schunck 1995)

Canny edge detector estimates the operator that optimizes the product of the signal-to-noise ratio and localization. The result from convolving the image with Gaussian smoothing filter using separable filtering is an array of smoothed data

$$S[i,j] = G[i,j;\sigma] * I[i,j], \quad (19)$$

where σ is the spread of the Gaussian and controls the degree of smoothing. The 2×2 first-difference approximation can be used to compute S[i,j] and produce two arrays for the x and y partial derivatives

$$P[i,j] \approx (S[i,j+1] - S[i,j] + S[i+1,j+1] - S[i+1,j])/2 \quad (20)$$

$$Q[i,j] \approx (S[i,j] - S[i+1,j] + S[i,j+1] - S[i+1,j+1])/2. \quad (21)$$

Further, the magnitude and orientation of the gradiant can be written as

$$M[i.j] = \sqrt{P[i,j]^2 + Q[i,j]^2} \quad (22)$$

$$\theta[i,j] = \arctan(Q[i,j], P[i,j]), \quad (23)$$

where the arctan function takes two arguments and generates an angle over the entire circle of possible directions. (Jain et al. 1995)

3.4.3 Corner detection

Corner detection is mainly used in motion detection, image registration, video tracking, image mosaicking, panorama stitching, 3D modelling and object recognition. A corner can be defined as an intersection of two edges. Harris and Stephens (1988) introduce Moravec's corner detection, where a grayscale 2-dimensional image I is used. Consider taking an image patch over the area (u, v) and shifting it by (x, y). The weighted SSD between these two patches, denoted E, can be written as

$$E(x, y) = \sum_u \sum_w w(u, v)(I(u + x, v + y) - I(u, v))^2. \quad (24)$$

$I(u + x, v + y)$ can be approximated by a Taylor expansion, and $I_x$and $I_y$are the partial derivatives of I. Further, equation (26) can be represented as an approximation

$$E(x, y) \approx \sum_u \sum_w w(u, v)(I_x(u, v)x - I_y(u, v)y)^2. \quad (25)$$

The response may be noisy and can be smoothened by using a smoothing window, for example Gaussian. The small change (shift in $E(x, y)$) can be written as

$$E(x, y) = (x, y)M(x, y)^T, \quad (26)$$

where $M = \begin{bmatrix} A & C \\ C & B \end{bmatrix}$. E is closely related to the local autocorrelation function with M describing its shape at the origin. Harris and Stephens give three cases:

"A. If both curvatures are small, so that the local autocorrelation function is flat, then the windowed image region is of approximately constant intensity (ie. arbitrary shifts of the image patch cause little change in E).
B. If one curvature is high and the other low, so that the local auto-correlation function is ridge shaped, then only shifts along the ridge (ie. along the edge) cause little change in E: this indicates an edge.

C. If both curvatures are high, so that the local autocorrelation function is sharply peaked, then shifts in." (Harris and Stephens 1988)

3.4.4 Morphological operations

Morphology operations are very versatile and useful as they can be used to alter the shape of spatial structures and the most used morphological operations are called dilation and erosion. The image that is processed can be defined as $g(r,c)$ and $s(i,j)$ is the image with a region of interest (ROI) S. The image s is called the structuring element.

The dilation can be achieved by using a Minkowski addition and transposing the structure element s:

$$g \oplus \check{s} = (g \oplus \check{s})_{r,c} = \max_{(i,j)\in S}\{g_{r+i,c+j} + s_{i,j}\}. \quad (27)$$

Minkowski addition is a sum of two vector sets, and Minkowski subtraction is a difference of two vector sets in n-dimensional space.

Typically, the structure element s can be assumed to be 0 (the flat structuring element). Then, the dilation has enlarging effect for the foreground, which means that parts of the images that are brighter than their surroundings are enlarged. Moreover, it shrinks the background, in other words the parts if the image that are darker than their surroundings. For example, the dilation can be used to split dark objects or connect bright objects to each other.

Same is done with the erosion, but the grey value erosion enlarges the background and shrinks the foreground. Erosion is the Minkowski subtraction for grey value images with the transposed structure element s:

$$g \ominus \check{s} = (g \ominus \check{s})_{r,c} = \min_{(i,j)\in S}\{g_{r+i,c+j} - s_{i,j}\}. \quad (28)$$

The erosion is used to split bright objects and to connect separated dark objects.

The morphological operations can be thought to be two special rank filters when flat structuring element $s(i,j) = 0$ is used. They can be referred to a minimum or a maximum filter as they select the minimum or the maximum value of within the domain of the structure element, which can be considered as a filter mask. This means that in the dilation every pixel value in the image $g(r,c)$ is replaced with the maximum value in the neighbourhood defined by the ROI, and in the erosion, the minimum value is used similarly to the maximum value in the dilation. Therefore, dilation is often considered as the maximum filter and the erosion as the minimum filter. (Van Droogenbroeck and Talbot 1996)

3.5 Light-emitted diode analysis

LEDs can be analysed by various different methods, for example with machine vision camera, LED analyser or spectrometer (Keyence Vision Systems; Feasa 2013). In machine vision applications LED analysis is integrated and LEDs are measured with colour camera. Captured images can be analysed by machine vision software. Colours can be detected from black background, and colour and intensity can be measured.

LED analyser measures the intensity and colour of LEDs. Analyser returns values for hue, saturation and intensity, when spectrometer measures the wavelength of the light, i.e. spectra, to detect colours of the LEDs. Every colour corresponds to a range of wavelengths. (Feasa 2013)

3.6 Industrial machine vision software

Various companies offer machine vision software and camera packages. Many of machine vision based cameras are provided with a machine vision software but software can be also purchased separately. Keyence, Optofidelity, National instruments and Orbis

systems offer machine vision and image processing software and applications. Moreover, Keyence and Orbis systems also offer camera packages when National instruments and Optofidelity have cameras from separate manufacturer such as Basler AG. Table 3 shows what software options these companies have.

Table 3. Industrial machine vision software.

Company	General	Machine vision	Software	Camera
Keyence	• individually customed set-up • manufacturing • R&D	• wide scale of image processing algorithms	• offers software • C-language • ready-to-use	• own camera series
National instruments	• data aqcuisition • instrument control • industrial automation	• wide toolboxes -> IMAQ • viual stuodio for machine vision	• IMAQ blocks • own toolboxes • user implements and creates own	• offers Basler camera and lenses
Optofidelity	• robot assisted testing • quality assurance	• calibration • locator • template matching • intensity measurement	• Labview toolboxes • DIT tool blocks • user implement them in own test environment	• suitable for many camera manufacturers
Orbis systems	• visual inspection devices • visual inspection softwares	• wide scale of image processing algorithms • Cognex vision blocks	• C-language • Cognex VisionPro machine vision software • ready-to-use • easy-to-use	• uses Basler camera

3.6.1 National instruments: LabVIEW

LabVIEW (Laboratory Virtual Instrument Engineering Workbench) is a system-design platform and development environment, which use graphical language G. It is visual programming language that can be used to acquire data from instruments, process data, for example with filters, analyse data and to control instruments and equipment (automation). (Larsen 2011)

National Instruments (NI) provides machine vision and scientific imaging hardware and software tools. These vision products can be used to solve various applications using image processing technology. For example, NI offers toolboxes and drivers for LabVIEW for machine vision applications. These features can be purchased individually for the needs of the application. (National instruments 2017)

3.6.2 Keyence

Keyence is the company in the field of the development and manufacturing of industrial automation and inspection equipment. It is working worldwide and their product selection includes code readers, laser markers, machine vision systems, measuring systems, microscopes, sensors, and static eliminators. Keyence is marketing their products in the manufacturing and R&D sector. (Keyence Corporate overview)

For inspection site, they offer machine vision, measurement systems, microscopes and code readers. These inspection products can be used either on an assembly line or in a laboratory. They offer machine vision systems that could be used in the HMI testing. Vision system products includes various types of series, which have different stages of camera and software. Furthermore, they offer lenses, lighting and other accessories to support the vision system. Although, the system is not individually customed. (Keyence Vision systems)

3.6.3 Optofidelity

Optofidelity is a technology company that offers hardware and software solutions for the manufacturing industry especially in robot assisted testing and quality assurance. Customers of Optofidelity include manufacturers of smartphones, tablets, laptops, automotive infotainment and industrial smart machinery (Optofidelity 2016). They provide different kind of production testing solutions, research and development testing solutions, and fully customize solutions for customer specified needs.

Optofidelity's products are based on machine vision and imaging. For example, they offer Display Inspection Tool (DIT) (Optofidelity 2012; 2013), which is visual inspection tool for LCDs and mobile phone displays. It promises automatical checking of the display content pixel by pixel, measurement of the contrast ratio against specification and verification of colors and intensities of complex segment displays. Prices of the products are not public as the solutions are customized.

In their website, Optofidelity introduces benefits why to use their software. First, they have the full spatial calibration feature, which corrects distortion caused by camera and lenses. Second, their software is simple to use, as the user needs to set up the camera and lens, adjust FOV, and grab three images from the display, after which the system is ready to begin inspecting the display. Thirdly, the software supports wide range of cameras and is NI LabVIEW compatible. (Optofidelity 2013)

3.6.4 Orbis systems

Orbis systems offers quality control and functional testing solutions and services for customers' research and development (R&D), production and after sales needs. Their services include engineering, prototyping and integration services. Their products are based on their own platforms, which contain test systems, radio frequency signal switching units, test fixtures and adapters, and software. Orbis systems has wide expertise from mobile phone manufacturing as it has worked with manufacturers such as Nokia. (Orbis system Homepage)

4. TESTING SYSTEM

In this chapter is presented the testing of the protection and control relays, the focus is in the testing system of HMIs. The upgraded set-up, which is called as the current system, is discussed in detail, and changes made are presented in the chapter 5. The original set-up, which was the set-up at the starting point, is upgraded with new camera and lens. Five adapters needed to be upgraded as all of them had been used with differing camera-lens set-ups and settings.

HMIs of 615 and 620 series are tested with the same adapter and 630 series has its own testing system. The focus is on test system of 615 and 620 series.

4.1 Testing of protection and control relays

The Relion® product family relays are manufactured and tested according to the ABB testing procedure. PCBA-suppliers carry out module level tests, and final products are tested in the ABB factories. The testing platforms are similar in ABB factories and PCBA-suppliers.

The testing platform contains a test adapter, a computer, power supply management and amplifier, a function generator, a controller unit, a multimeter and test software, which is identical in every manufacturing level to ensure a uniform quality of testing. A function of every module is tested individually in PCBA –suppliers with specially developed test adapters. There are various modules, such as HMI, central processing unit (CPU), communication module (COM), binary input/output (BIO) and power supply module (PSM).

The testing procedure is presented in figure 9. In final assembly phase, all needed modules are added to a final product. Module labels with serial numbers are attached to the relay case, and read to save the data with relay identification and customer information.

The assembled product goes through high potential (HiPot) test, in which high voltage is applied to the product and leakage current is measured. If product passes the HiPot test, it can be thought to be safe in ‘normal’ conditions. After HiPot test, product will go through final functional test, which includes initial tests, software download and module tests. From final functional test, the product is placed to the burn in chamber for 12 to 24 hours depending on the product type.

The HMI is verified in final functional phase with visual inspection. Operator checks LEDs and LCD by naked eye. In addition, proper function of the HMI is checked after test run in burn in chamber.

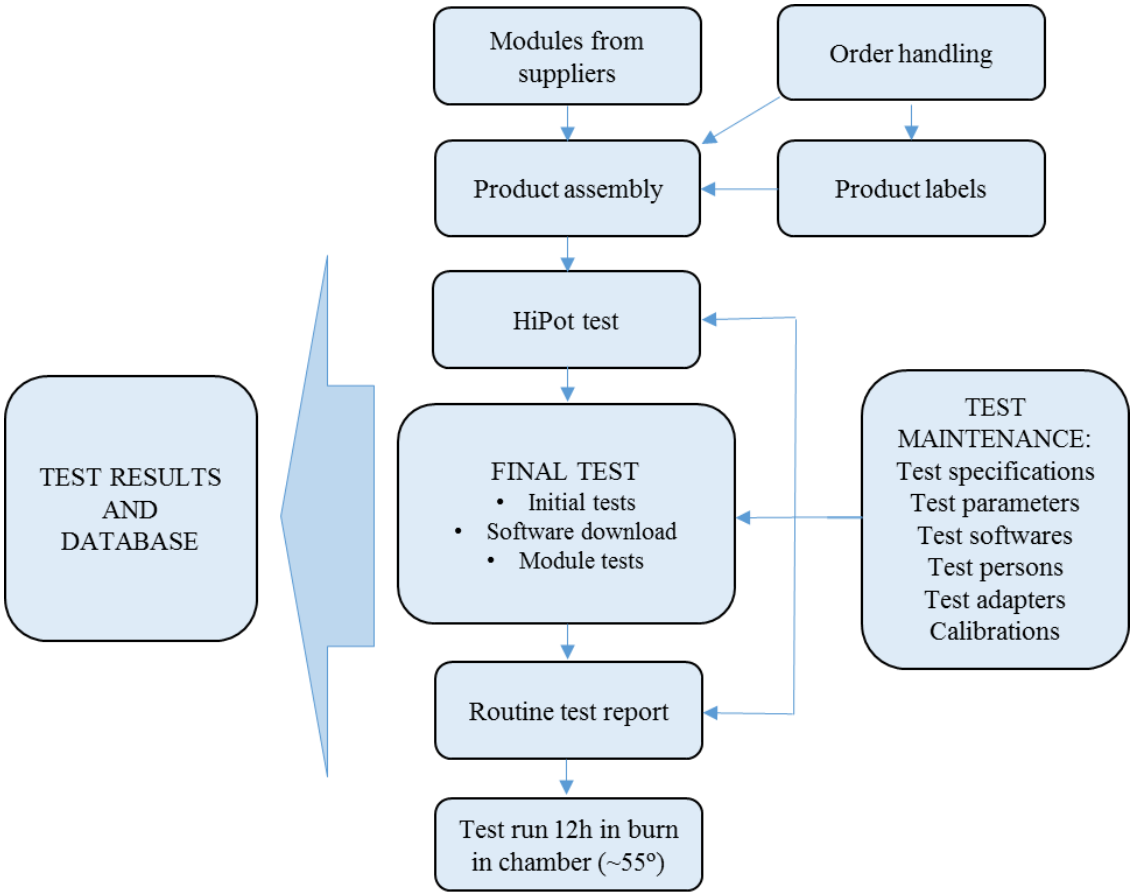

Figure 9. Flow chart of assembly level tests.

4.2 Human-machine interface module testing

HMIs are manufactured and tested in PCBA-suppliers to ensure quality of the products. The HMI test sequence consist of 15 subsequences (Appendix C), of which we are focusing on LCD test. The visual inspection of HMI contains checking of LCD dead pixels, bitmap comparison, and intensity measurement. Dead pixels or errors in bitmap image should not occur and LCD intensity should stay in tolerance values so that printings are readable.

4.2.1 System requirements

Every relay model has been given specifications for its function. In the 615 series, HMI specifications include two LCD sizes, 128×128 and 65×128 pixels. Furthermore, LCDs in the series are black and white displays. (ABB 2016)

Requirements for the camera are that it can take still image in grey scale from two different display sizes. The different sized displays have different lighting properties, and the system should be able to measure both of these. Furthermore, the illumination of the LCDs vary within the same model. System should be able to measure all LCDs that are determined to be within the tolerance values and which should pass the tests.

There are no special requirements for the lens in this application. The lens should be suitable for the camera sensor size and resolution, which are often used and manufacturer offers lens compatible with the camera. The distance to the material is small, which can be problematic, when high image quality is needed, as pixel size resolution is desirable. Moreover, high speed is not required as one still image is taken at the time, and the object is not moving.

The software should be able to detect defect pixels from a captured image, verify that the desired image is printed on the LCD display, and measure the intensity of the LCD. Machine vision software manufacturer has given requirements for the measurement

system. The resolution of the camera and the sensor should be four times the smallest detail in the target image.

4.2.2 Test station and adapter

The HMI test system of protection and control relays of 615 and 620 series contains tests for features of the HMI, which are display, LEDs, buttons and software. In this thesis, the focus is in the tests of the visible functions of the HMI, which are tested with machine vision application.

The HMI test adapter includes the HMI testing bed, a camera to measure the function of the LCD, a LED analyser and pushing rods for button testing. Camera is mounted at the top of the adapter. The adapter cover plate (pressing plate) can be opened in order to get the HMI inside the test adapter. Test adapter is presented in Figure 10. The adapter co not include light source, and ambient light is reduced by camera case. The only light source in the system is the LCD.

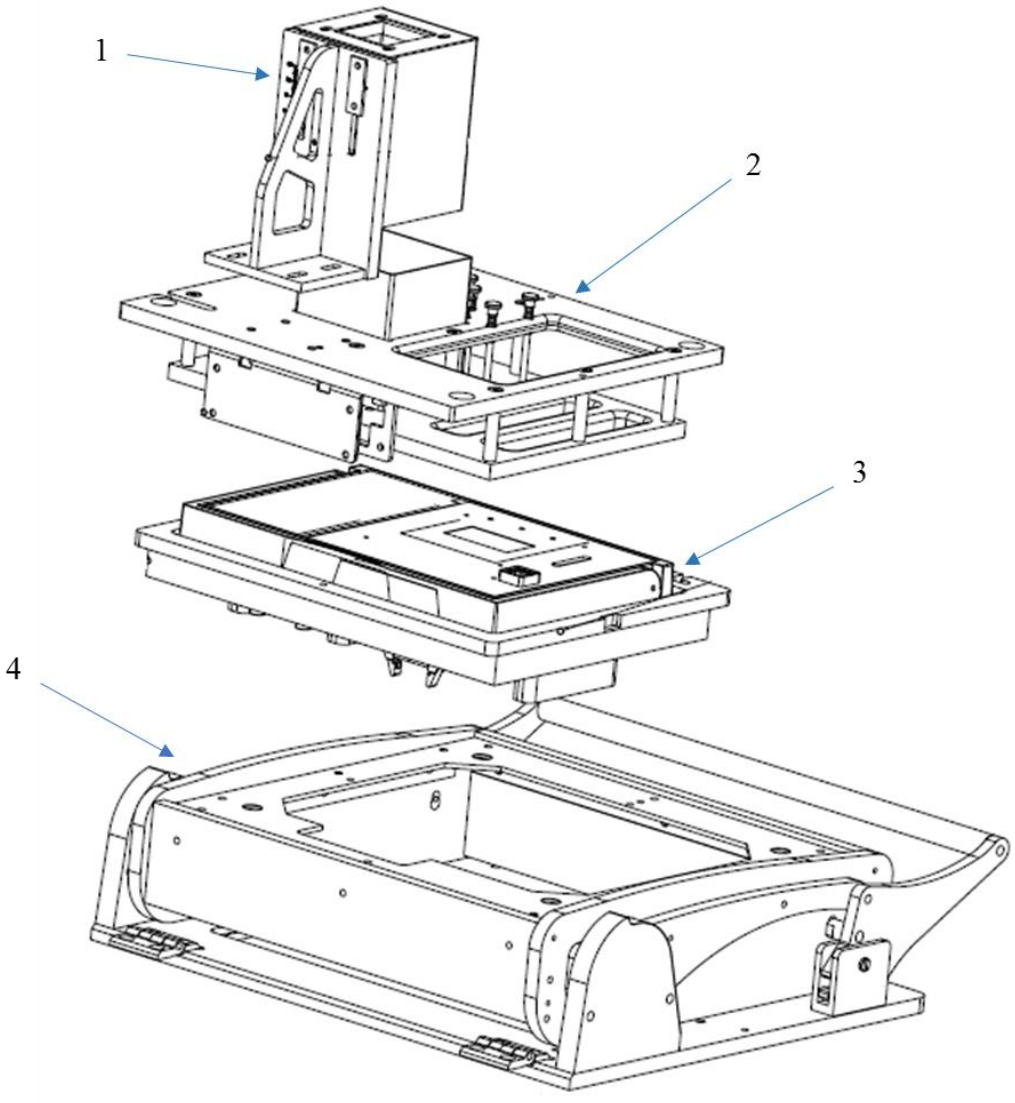

Figure 10. 615/620 HMI test adapter. 1) Camera stand 2) Pressing plate 3) HMI testing bed 4) Adapter body

630 series test set-up consist of test station, a computer, and machine vision camera and software. The software and device differs from 615/620 series set-up. The machine vision operations are build-up in the industrial software, and user must decide which operations to use. Software includes basic machine vision operations, such as ROI location, intensity measurement, template matching, and particle detection. The operations are listed and user can choose right operation to implement them into the measurement. In software, the user navigates with remote, which is delivered with the software and camera system. The

camera is connected to a small computer, which includes drivers and software, so the main computer is needed to save images and to connect the system to the main network.

The system includes two cameras: colour camera and monochrome camera. The monochrome camera is used to image and measure the function of the LCD and the colour camera is used to measure the function of the LEDs. LED measurement is more accurate than with the 615/620 series adapter.

4.2.3 Camera and lens

The original 615/620 HMI test set-up included Firewire-camera and Pentax-lens. The work was started at the situation that only one adapter has the current camera and lens, but with unstable function. All adapters should be upgraded to the current set-up, where camera distances from the lens and the target are strictly determined. The distances should be determined by using focal length, the size of the target and the sensor.

A monochrome GigE (Gigabit Ethernet) camera with charge-coupled device (CCD) sensor is used (Appendix D). GigE cameras use GigE Vision standard that is a global camera interface standard for fast and low cost communication protocol (GigE Vision standard 2016). Resolution of the camera is 1296 pixels x 966 pixels, when sensor delivers 22 frames per second at 1.3 megapixel resolution. Lens, which is used has a focal length of 4 mm, aperture range of F1.8-F22 and minimum working distance of 100mm. Figure 11 illustrates the camera set-up.

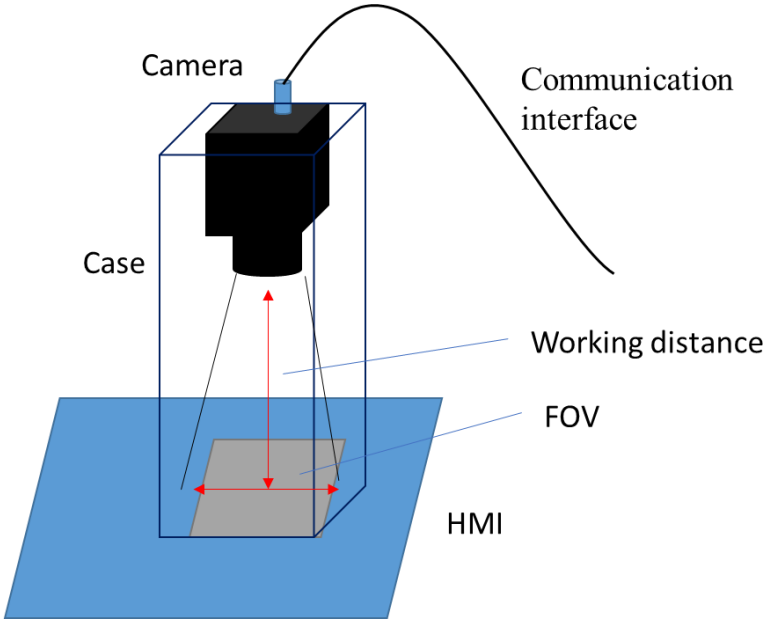

Figure 11. Camera system. Camera is located inside the case, which reduces light. Working distance and FOV are illustrated.

4.2.4 Light-emitted diode analyser

Intensity and colour of the LEDs are tested. A LED can be green, red, or yellow depending of its semantics. A green LED represents good function of the relay when a red or yellow LED represents dysfunctionalities. Tolerance values are set for colour and intensity, in which individual LEDs should stay.

In the current test system, Feasa LED analyser is used (Figure 12.). It contains 20 fibres, which collect light from LEDs. It measures values of intensity of every colour (green, yellow, red) that LEDs show. Fibres are set inside the adapter and their optical heads are set into the alignment plate as seen in Figure 13. The adapter set optical heads tightly on top of the LEDs of the HMI. Analyser channels are adjusted, and gain is set for every fibre individually.

The analyser uses serial port to connections and data movement, which connects up to 30 LED analysers. External trigger is used to synchronize measurement with the desired

event. Analyser starts to measure when LEDs are driven into preferred state, such as green or red colour mode. Furthermore, test time depends on the intensity of the LEDs being tested.

Figure 12. Feasa LED analyser. (Feasa 2013)

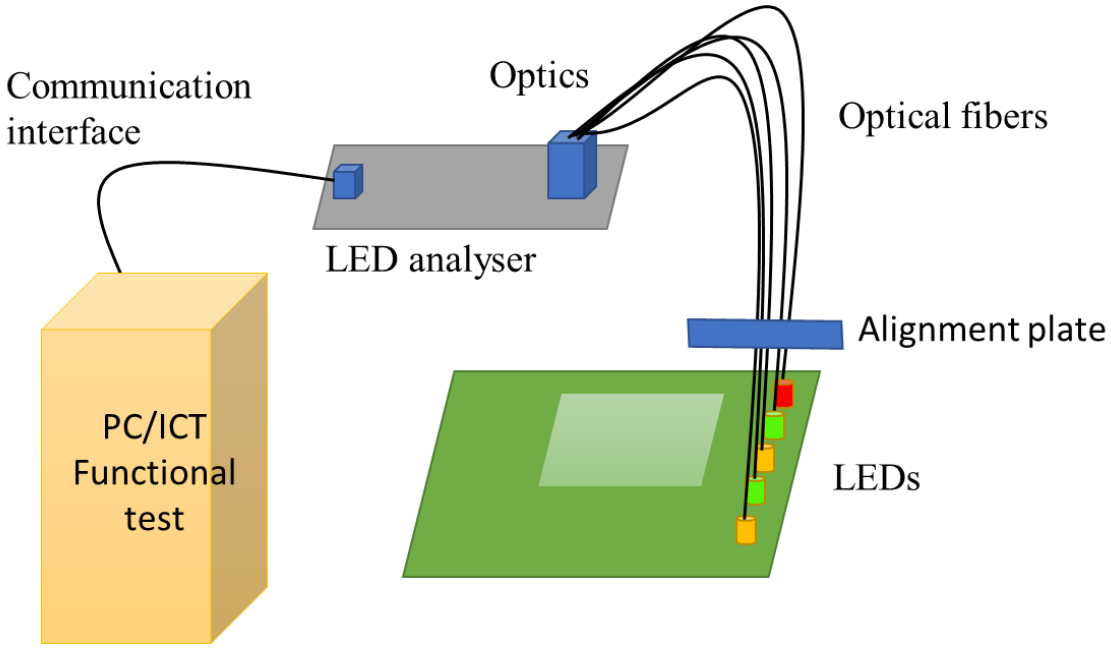

Figure 13. Illustration of LED analyser set-up. Alignment plate is integrated to the adapter case in bottom of pressing plate.

4.2.5 Software

Programming language, LabVIEW, is used to carry out the HMI test algorithms. Mostly, all test software are developed at ABB, but machine vision parts of the HMI test contain parts from supplier. Goal was to get better understanding of the machine vision tasks, and how they could be used efficiently.

The LCD test sequence contains of initial phase, where camera and connections are checked, testing phase, where functional tests are carried out, and closing phase, where all connection are closed. Settings used in upcoming operations are set in initial phase depending on the LCD size. Test images are captured and processed in testing phase.

Machine vision operations of the LCD test can be divided into five groups: spatial calibration data, ROI definition, defect pixel inspection, bitmap comparison and intensity measurement (Figure 14). The LCD test needs three images: all pixels off, all pixels on and image with desired graphic, in this case text ‘ABB’ (Figure 15). For further processing, the images are converted into 2D-arrays of unsigned 8-bit integers. Intensity of the pixels is presented between [0,255]. These images are calibrated and processed images are used in defect pixel detection and bitmap comparison.

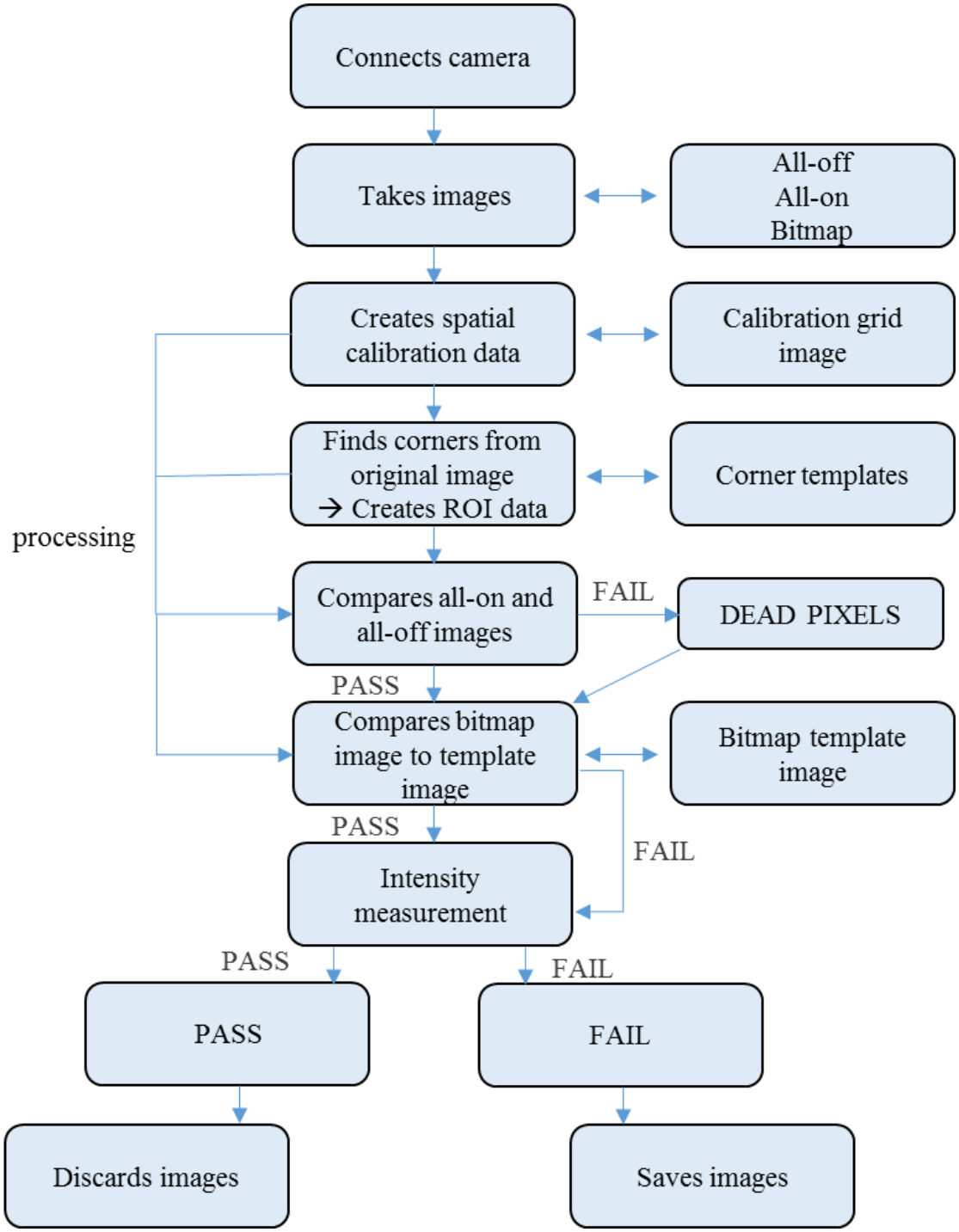

Figure 14. Flow chart of the LCD test.

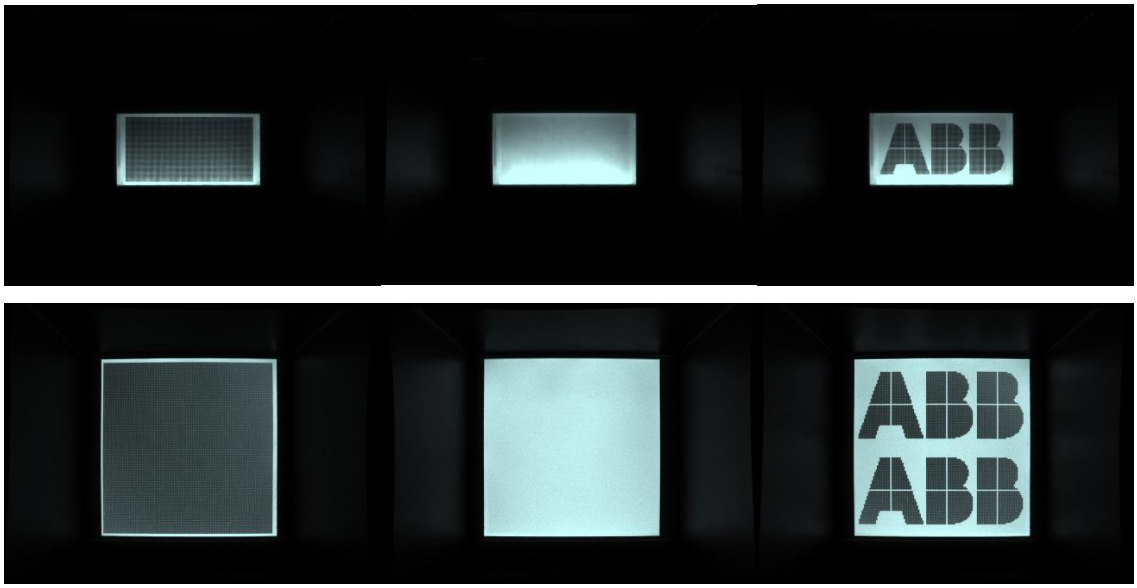

Figure 15. Images needed in LCD testing. Top left) All-on image. Middle) All-off image. Right) Image with ABB text of small LCD. Bottom left) All-on image. Middle) All-off image. Right) Image with ABB text of large LCD.

Images are processed with spatial calibration, which reduces a distortion cause by camera and lens. Unprocessed images contain barrel distortion that can be seen as distortion of a LCD edges (Figure 16.). Dot image (Figure 17.) is used to create a spatial filter image (Section 5.2). Image of the dot image is captured with the camera and the width between two dots at the centre of the dot grid image is measured, as there should be minimal distortion. The result is used to scale the widths of rest of the dots to be identical. Once the calibration is done, it can be used to process images captured with identical camera and lens set-up.

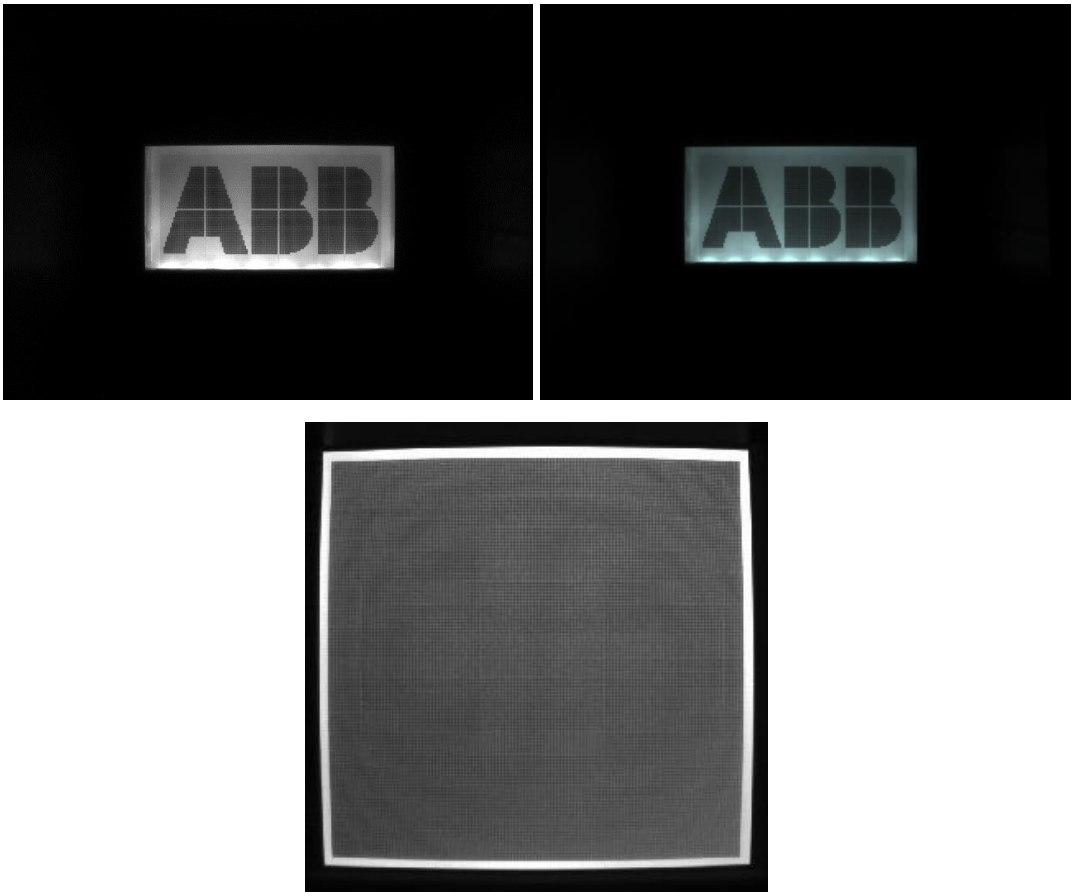

Figure 16. Comparison of original and processed images. Left) unprocessed image from camera. Right) processed image. Bottom) unprocessed image from camera.

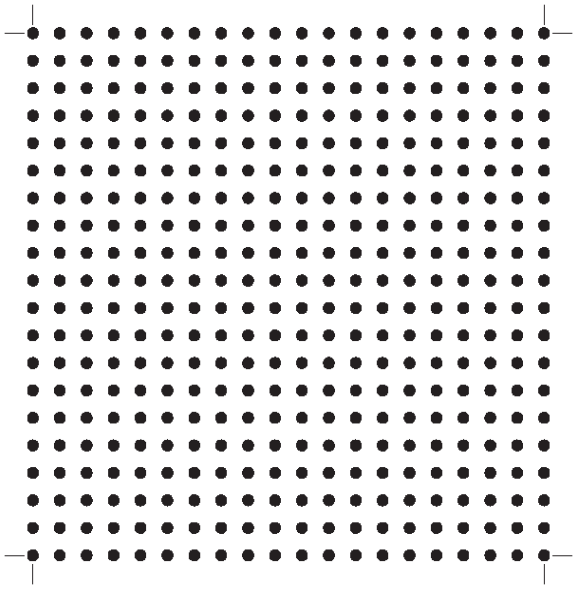

Figure 17. The dot grid image is used for a geometrical calibration. Here, the picture is zoomed out.

ROI, or LCD display, is identified from captured image by using corner template images (Figure 18). Each corner has template that algorithm tries to find from the image. Corner points found are written into a matrix for a further use. ROI area is determined with top-left and bottom-right corners by constructing rectangle, which is used in analysis.

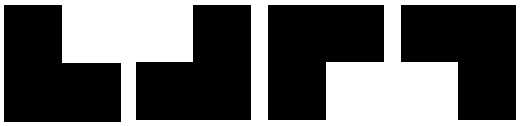

Figure 18. The corner templates images for each corner.

Defect pixels, both hot and cold pixels, are detected by using processed all-on and all-off images. LCD can have defect pixels which can be separated into hot or cold pixels. Defected pixels are pixels that are stuck in some stage. Hot pixels are stuck to be on even they should be off and cold pixels vice versa. The minimum difference between pixel intensities is calculated, and if difference is below threshold, pixel is detected to be defect. Software marks all pixels individually to be normal pixel, cold pixel or hot pixel depending on in which image pixel is detected. Pixel is normal if measured difference is over the threshold, cold if difference is found in all-on image and hot if difference is found in all-of image.

Edge and middle pixel area in LCD display have different threshold values. Edge is determined to be two pixels wide and the difference is defined to be smaller than in middle area pixels (Figure 19). That is because the light may reflect more into edge pixels than on middle pixels, so there is a spatial intensity variation. In the original system values for edge area (pixellimit_out) are 15 for large and 5 for small LCD, and for middle area (pixellimit_in) are 30 for large and 20 for small LCD. These values are also used in the current system, although their accuracy is estimated and additional investigation suggested.

LCD	small	large
pixellimit_in	20	30
pixellimit_out	5	15

Figure 19. Illustration of the middle and the edge area of the image, which have detection thresholds of pixellimit_in and pixellimit_out. The edge area is shown by red arrow and orange box and middle area is shown with green arrow.

In bitmap comparison, programmable test image is loaded to LCD, of which the camera takes an image. Captured image and template bitmap image (Figure 20.) are placed in a bitmap cluster. Similarity analysis is done according to the cluster, pixel by pixel. Defect recognising has threshold, which defines the percentage of pixel errors that are accepted. In the current system pass limit is set to be 0, which means any defect is not accepted. error pixels are collected to a boolean array, where True == defected pixel and counter starts from the top left corner at point (0,0). Defected pixels are marked to the original image by creating 2D array with original processed test image and additional defect visualization information. Defects are visualized by rectangles around the defect pixels. Same defect visualization method is used with hot and cold pixels.

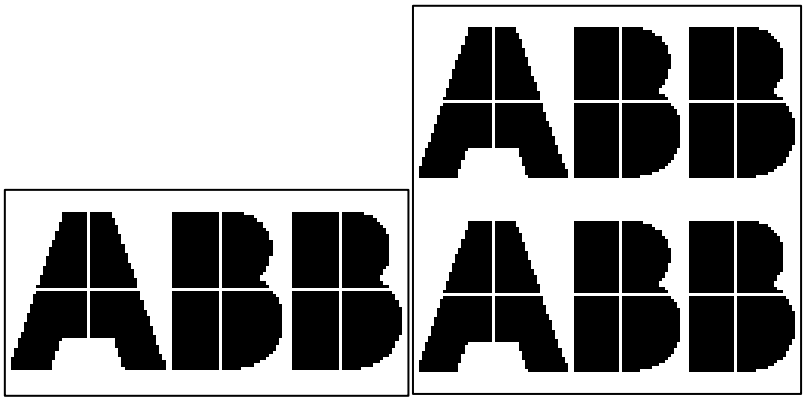

Figure 20. The bitmap template images for the small LCD and the large LCD, respectively.

Intensity of the LCD is measured over the ROI area. ROI data is used to define an area where intensity is measured. Unprocessed test image is used so that processing do not influence to the intensity values. LabVIEW contains ready-to-use block for intensity measurements and intensity is measured between [0,255], but it is not absolute value. If absolute value is desired, 3D –array with 0-value array and 255-value array should be created to normalize intensity. Tolerance for intensity is set to be 100-210 for large and 50-150 for small LCD. These values have been in use in the original system and are now used for the current system.

If defect pixel/pixels are found, follows error. Software do not give fail before it has run all steps in on test sequence (LCD test). Dead pixel detection gives error, which will follow during the next steps, but allow them to be done. At the end, test gives ‘Fail’, ‘Fatal fail’ or ‘System error’ depending on type of error. Processed test images (all-on, all-off, text image) with and without defect visualization are converted from 2D array and saved as PNG-image, if error occurs. Processed test images without defects are saved temporarily.

4.3 Fails in human-machine interface testing

The tests are done because of dysfunctionalities in HMIs. Even though real fails are rare, FPY is not as high as within other modules. Faults such as defect pixels in LCD, differences in LED intensity or colour, Ethernet connect and LCD voltage fails occur in daily basis. Many other fault types exist and a list of them is shown in Figure 21. All of them are not real product issues but rather caused by the test software or hardware limitations, or operator errors. These results are from two-month period.

The original system needs improvements because it detects false defect pixels, which means the pixels with normal functionality, but which are detected as defect pixels (Figure 22). These limitations are unknown and changes in the software and hardware are needed to decrease the number of negative faults. More examples of faults are shown in Figures 23, 24 and 25.

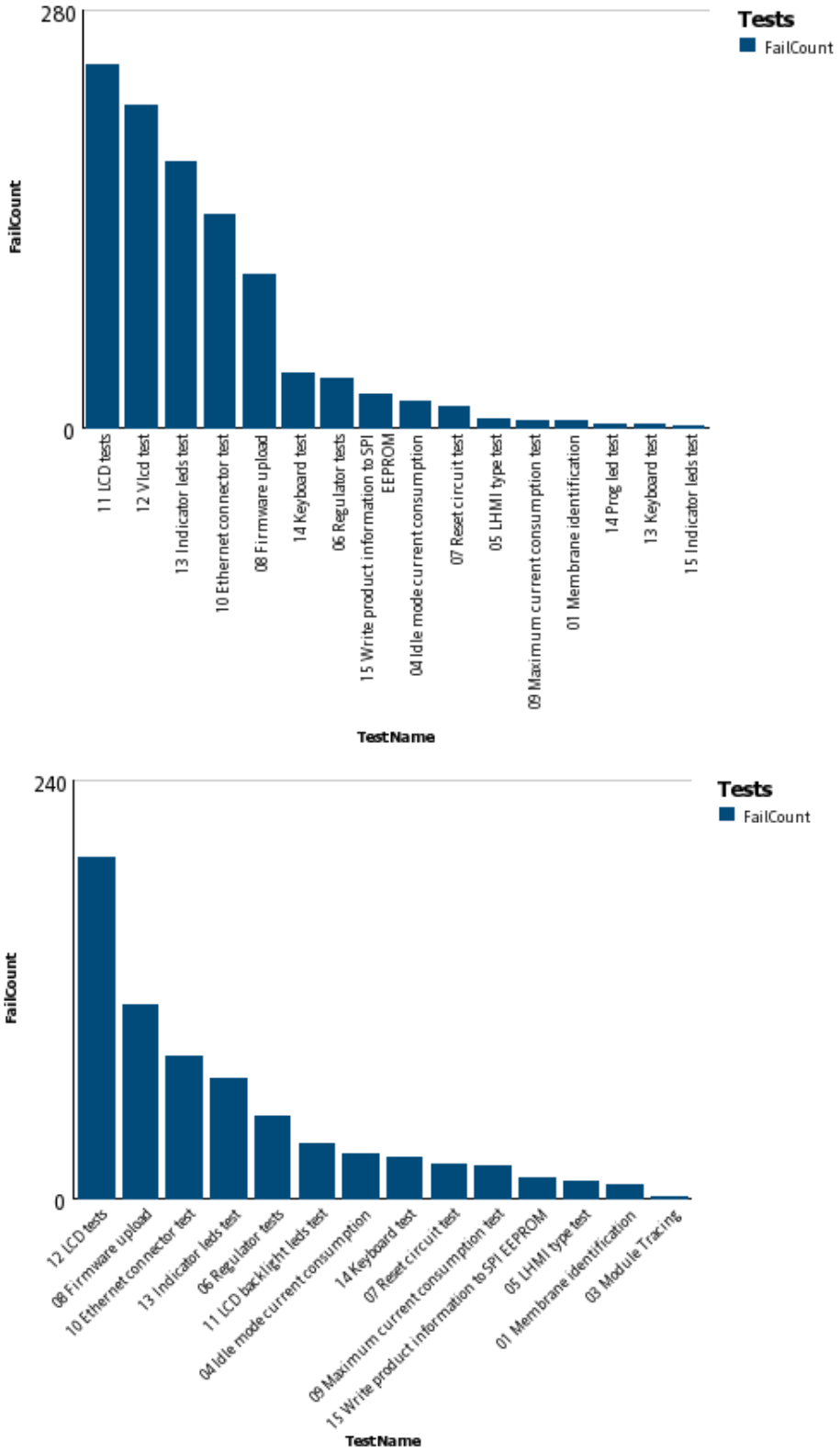

Figure 21. Fails in HMI testing with original set-up in two-month period. Top) Large LCD with 10002 tested products. Bottom) Small LCD with 5473 tested products. (ABB database)

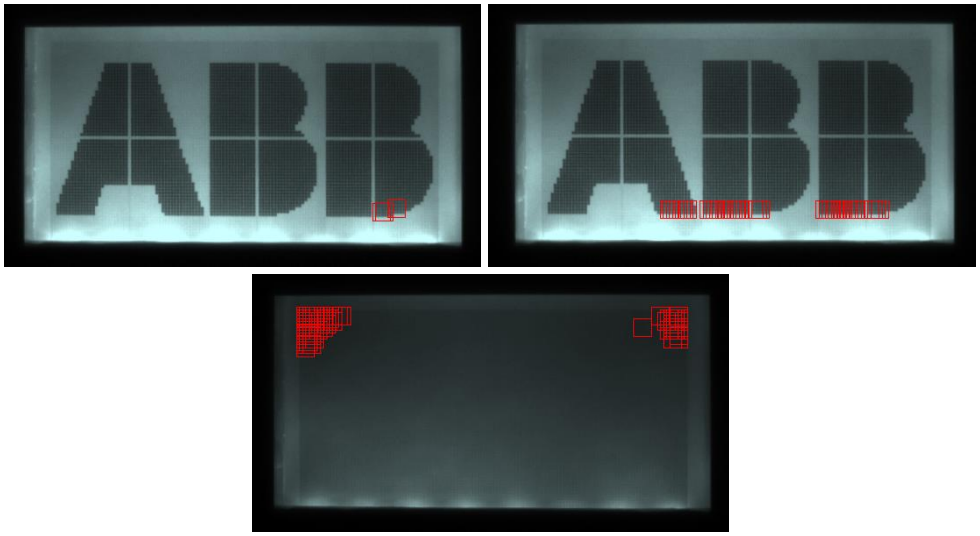

Figure 22. Images with false fails. Detected fails are marked with red squares. In these images, black area around the images is cropped. Top) false bitmap errors are detected. This is caused by high intensity of the LCD, which causes distortion of processed image. Bottom) false error, which is caused by the uneven illumination over the surface.

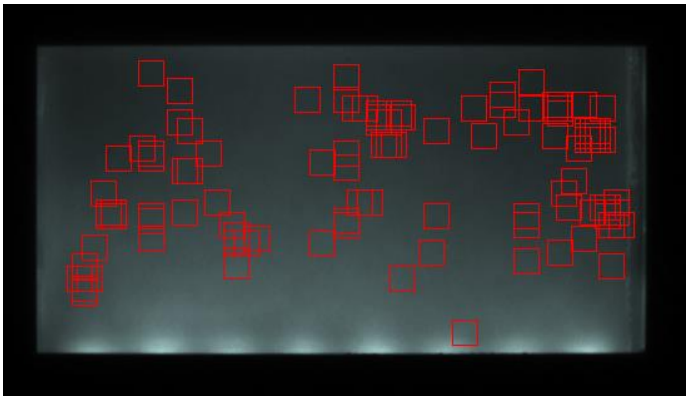

Figure 23. Image with dead pixels. Any of the pixels in the image are not functioning, which can be because of error in LCD drive or error in pixels.

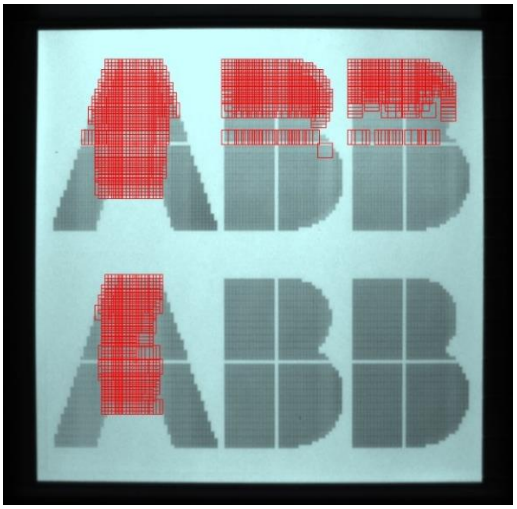

Figure 24. Bitmap image with low intensity pixels. Pixels, which intensity difference is out of the threshold values are marked with red squares.

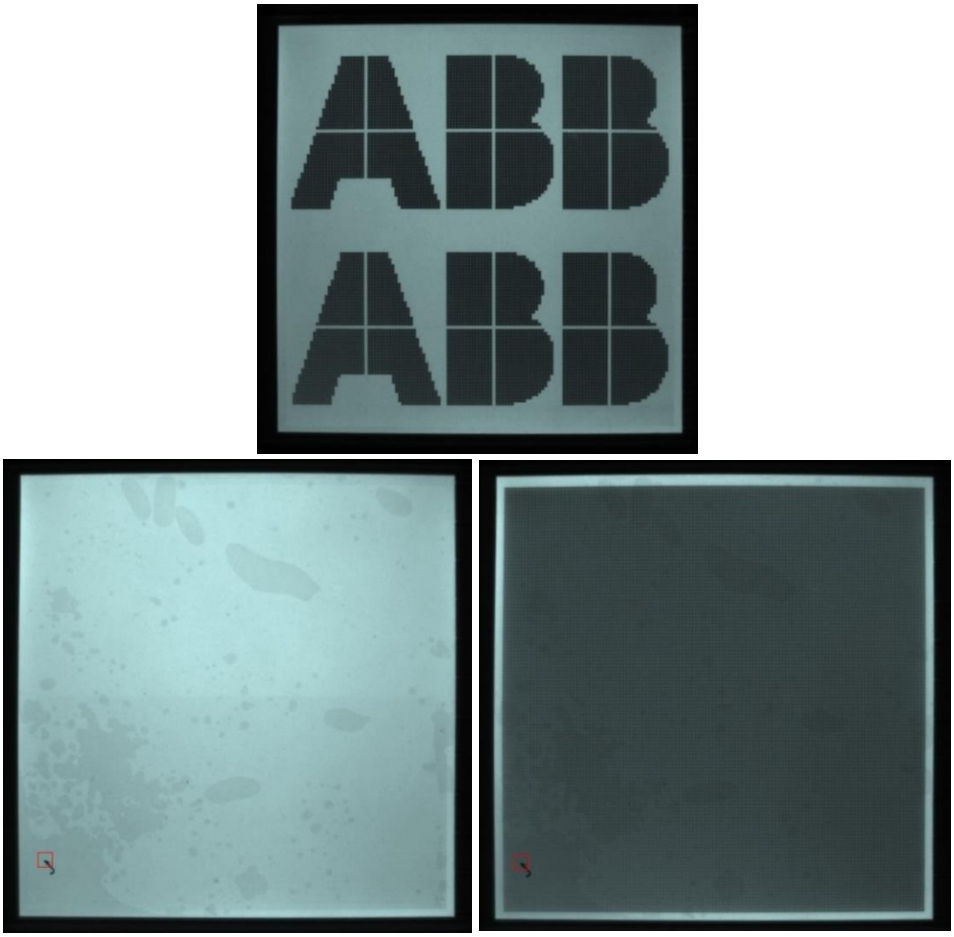

Figure 25. Detected faults on a large LCD. In these images, black area around the images is cropped. Top) the intensity of the LCD is too small. Bottom) Trash (hair, dust, etc) on the display.

Edge detection has been a problem in HMI testing. It causes loss of pixels and leads to a fail of a tested product. It may be the consequence of the low contrast between the pixels and the LCD material. Especially very bright LCDs cause problems with ROI detection, which leads to the distortion of the processed images (Figure 26) and further, fail of the product. After image processing, LCD should be located in the middle of the image area with straight edges, as illustrated in Figure 16.

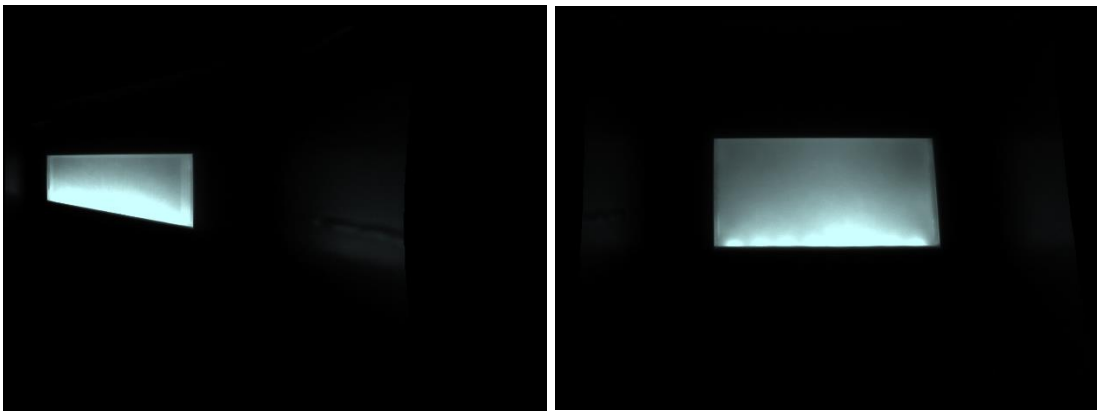

Figure 26. Examples of distortions caused by high intensity of a LCD. Black area around LCD image is showed for better demonstration.

5. UPGRADING AND TESTING OF THE SYSTEM

In this section, we present the changes, which were made to improve the system. The changes included new camera and lens, and their adjustments, new exposure settings, and spatial calibration. Evaluation of detection tolerances in software and overall function of the system are presented in the end of the section.

5.1 Camera and lens upgrade

New camera and lens were installed and adjusted to be suitable for HMI test measurements. Previously, distances of the camera, lens and target has not been calculated. For the current system, calculations were done and they were used to set camera and lens to the right position. The focal length of the lens is 4mm and the size of the large LCD is 64×64mm and the small LCD is 26×52mm. By using these values and equations (4), (5) and (6), the working distance can be estimated to be 82mm, when the size of the sensor is 4.86×3.62 mm. Because the minimum working distance of the lens is 100mm, we set the working distance to 100mm, which is about 22 in scale of the camera stand. With focal length used, the size of the image is estimated to be 129 × 96mm. Both the large and the small LCD fit in this imaging area. However, there will be more empty/black area than in the original set-up, but it will not affect the result as much as a wrong working distance.

Aperture was set to the aperture stop about f/3, which was mentioned to be the optimal aperture of the lens system (Appendix D.). This cut the intensity in captured images, as a smaller aperture reduces light, and thus the intensity of the image. To change intensity levels, gain and exposure time, which are controlled from external setting file, were adjusted. Effect of change of the aperture was tested (Appendix B) and in Table 4. and Table 5. can be seen the measured intensity differences between the original system and the current system. Two LCDs were used as an example, and from the histograms and plane plots (Appendix B) can be seen the differences caused by the change in aperture size. With large aperture, intensity increases and the histograms show that the intensity is

more near to the value 255, when with the small aperture, intensity approach value 0. In plane plots, increase of grey values can be seen from smaller to larger aperture.

Because of changes in aperture size, the exposure time was adjusted. Gain must be as small as possible, so it was not changed. For small LCD gain was set to 430 and for large LCD 350. The difference is because of variances in backlight intensity. Gain can be defined to be the measure of higher sensitivity to light, which means that when gain is increased it will increase apparent of light over the image with the selected exposure. Small LCD needs higher gain because of lower backlight intensity.

Position of the camera and aperture size affect to the focus of the image, which was adjusted after camera and aperture locations were decided. Focus control of the system is manual and can be made by moving the focus ring of the lens.

5.2 Spatial calibration

Spatial calibration is important part of the image processing in this test system. It reduces lens distortions and can be used to calibrate image pixels into the real-world units. New calibration grid image must be taken because of the changes in the camera set-up. Incorrectly taken calibration image and wrong implementation produce useless images.

In this work, a new calibration image was taken and calibration was implemented, and they should be used with the current system. 50% zoom-in was used for the original dot grid image from LabVIEW (Figure 17.). The dot image was printed into a transparency, which was then set on top of an HMI's LCD. The camera distance and lens position should be set the same with the test measurements. Thus, camera position was moved 3mm up, so that working distance stays constant, as the LCD surface is located 3mm under the HMI surface. Camera settings, gain and exposure time, are adjusted to get unsaturated and sharp image. The calibration image must be taken with the image size of 768×1024 pixels and saved in BMP-format because the size and format is used when checking calibration validation. After validation check, the image is extended to size

966×1296 pixels. The extended BMP image is converted to PNG image so that it can be used by the LCD test calibration block.

Calibration image must be verified before use. The image is compared to a verification grid image, which contains straight lines (Appendix E). Validation shows how effectively calibration corrects distortions. The calibration chosen for the current system has decent validation, as it is similar with the calibration validation accepted by developers of the software (Appendix E). After validation, the captured grid image is converted to PNG format and resized (1296×966) to match with the camera format. If the size or format of the calibration grid image is wrong, the result is error in software.

Software is changed to be suitable with the calibration image used. There is a matrix that must be changed to be equal with the calibration image (Appendix E). Matrix contains corner values of four squares, top-left and bottom-right from each, which constitute the real calibration image. If corner points are located incorrectly, the calibrated test image will be critically distorted (Figure 27.).

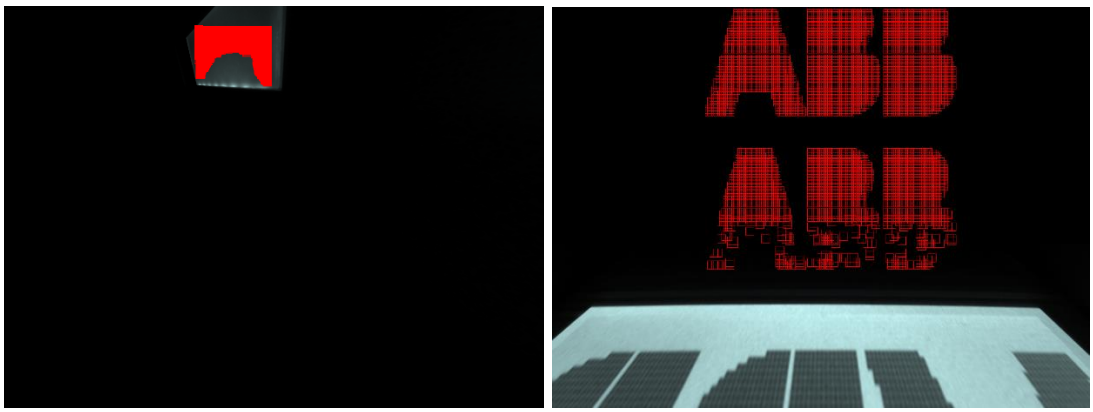

Figure 27. Test images captured with incorrect corner values in the calibration matrix. Changes in matrix values produce various distortions.

5.3 Software tests

The function of the adapter and camera was tested. Resolution, edge detection and camera settings were tested and evaluated. In this chapter, testing of function of the current system is presented.

The camera settings were tested by changing the settings one by one. First, the gain was set to as small value as possible. The large and small LCDs have different values caused by the backlight of the LCD. Second, the exposure time was set to the value, which gives an unsaturated but bright and clear image. In Figure 28 is shown saturated and unsaturated images of the large LCD.

Exposure time is the time when the camera sensor is exposed to time. Longer exposure time will produce increase of intensity of the image. Exposure was tested with LCDs with different backlight properties to clarify the intensity scale, which should be accepted. The LCDs were evaluated by naked eye before inspection to make sure they meet intensity standards. Example of the intensity difference between LCDs can be seen in Figure 29. If the exposure time was too long, the image will be saturated, or as with the small LCDs, the image may be also distorted (Figure 26). Too short exposure time produces dim images with decreased intensity, which can cause fails in intensity test (Figure 28, Bottom) or negative faults in small LCDs (Figure 22, Bottom). The exposure time was adjusted individually to both small and large LCD. Adjusted exposure time for small LCD is 16000, when for the original system, it was 12000. Moreover, adjusted exposure time for large LCD is 12000, when for the original system, the exposure time was 10000.

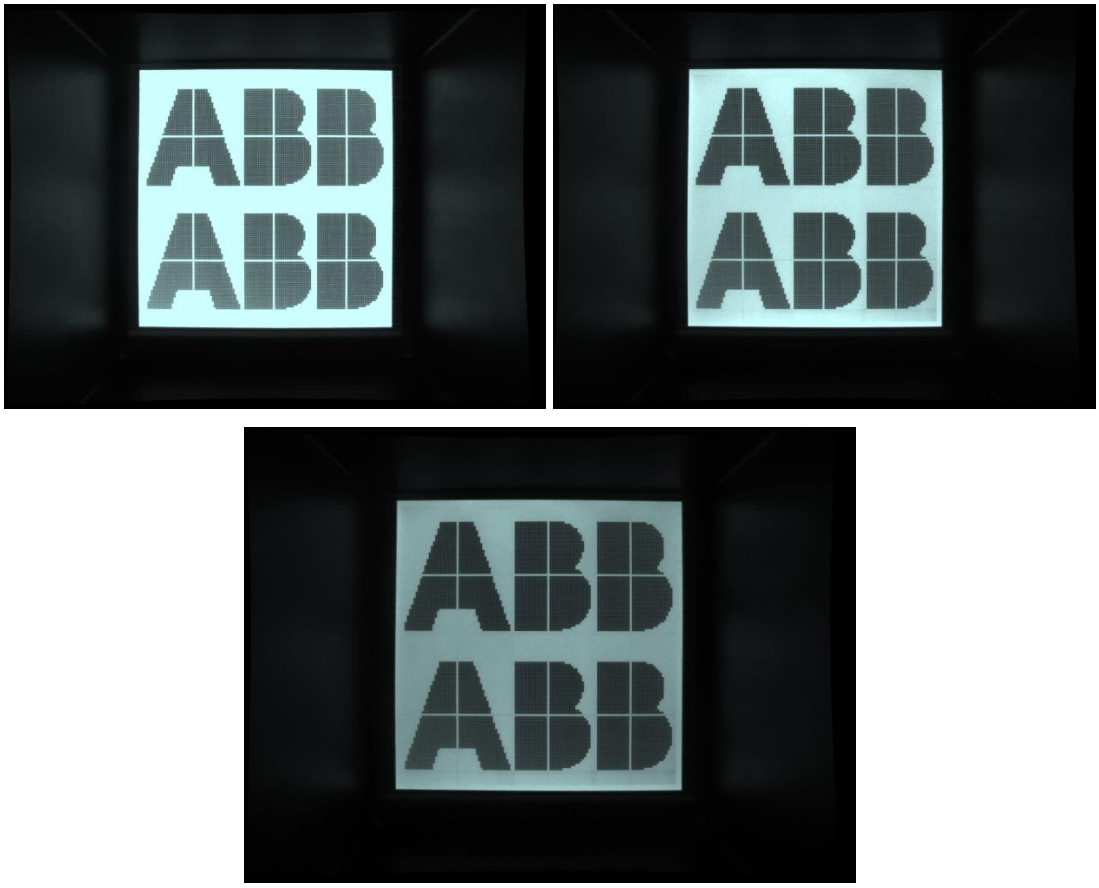

Figure 28. Illustration of changes in camera lighting settings. Top left) Saturated. Top right) Unsaturated, Bottom) dim image of a large LCD.

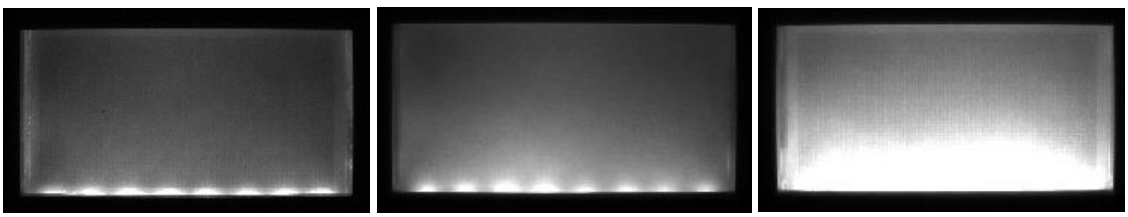

Figure 29. Comparison of unprocessed small LCDs. Images are captured with same exposure, and intesity difference caused by backlight LEDs can be seen. Exposure time 16000.

The camera and software detecting accuracy was tested by simulating dead pixels and thrash on the LCD. Coffee grounds were used, and example of the technique is presented

in Figure 30. Originally, pieces of paper were tried, but it was challenging to get small enough piece to simulate pixel size defects. Furthermore, paper transmits light, and hence, produces no simulation of the defect pixel. Coffee grounds do not transmit or reflect light, so they do simulate defect pixels and thrash.

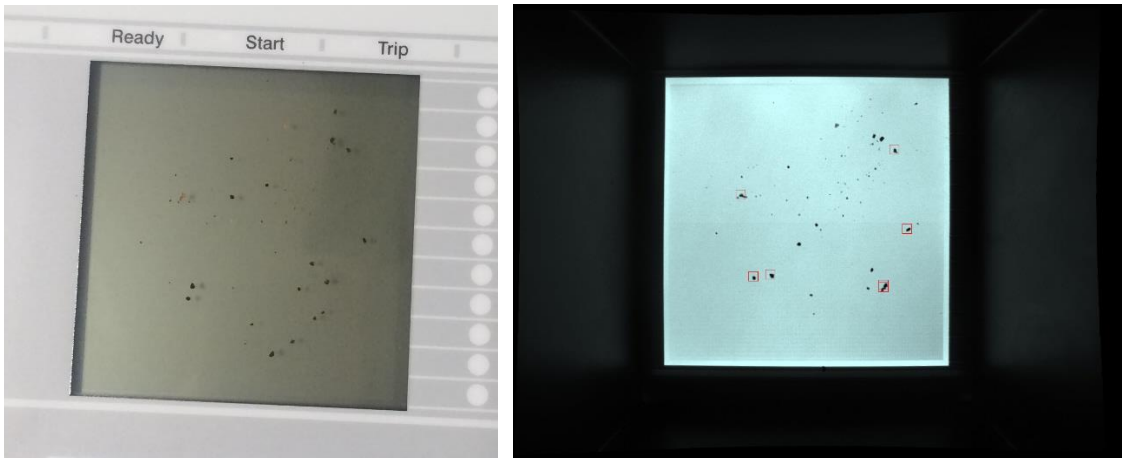

Figure 30. Coffee ground on the LCD panel. Left) by naked eye. Right) as seen by camera.

First, large coffee grounds were used to test defect detection. Large particles were detected both in small and large LCDs. We evaluated detection accuracy by naked eye from images, and noticed that increasing the threshold value of the middle area gives more accurate detection compared to the original threshold values. When increasing the threshold more, the application starts to find negative defects. These are shown in Appendix A.

When increasing the threshold value of the edge area of the large LCD, it does not affect the middle area where the coffee grounds are. Even with values pixellimit_out 50 and pixellimit_in 30, and pixellimit_out 80 and pixellimit_in 20 the application does not detect the negative faults around the edges. The result image is similar to the Figure 1A (Appendix A). The middle area threshold can be increased to the value of pixellimit_in 120, when pixellimit_out is 15 without negative faults. However, when increasing both values greatly, negative faults are detected. Using values pixellimit_out 80 and

pixellimit_in 120 negative faults occur. From this can be concluded that threshold values can be changed to get more accurate results but the final values need more testing.

With small LCD, increasing of threshold values gives negative faults fast. Value of pixellimit_in 35 and pixellimit_out 10 give the result that does not include negative faults, but when increasing threshold more, negative faults occur. This may be caused by backlight properties of the small LCD, as the top corners are detected first, when increasing threshold values (Figure 10A).

5.4 Adapter similarity test

All adapters need to be upgraded identically with the new camera and lens. At the same time, camera position and settings are set as mentioned in previous sections. At first, two adapters were upgraded to the new set-up, and the similarity between them was measured. For example, intensity values from first upgraded adapter are user as a baseline. The camera position and lens aperture stop do not have scales, which could be used to make two adapters identical, so the adapter function must be tested manually. Camera positions are set as identical as possible, as well as the aperture size. Finally, the similarity is tested.

Similarity of the adapters is tested with ten HMIs with large LCD and ten HMIs with small LCD. Test HMIs are from assembly line, so they have passed all the tests once in PCBA-supplier side. All LCDs were tested twice during the test, once with both upgraded adapters. The adapters overall function is tested at the same time as 20 randomly chosen LCDs are tested for adapter similarity. The sampling is small, but later, the adapter function is tested at HMI production. Intensities of the LCDs, measured by two separate adapters with similar set-up in the same test station are shown in Table 4 and Table 5 (Appendix F).

The decreased intensity value is due to the smaller aperture. This do not have effect to the brightness of the real LCDs, but leads to the adjustment of the intensity thresholds.

To get real understand of the suitable thresholds, production data is needed. After that, new intensity thresholds can be set.

The calibration sheet may have been useful, but as we wanted to compare the intensities between the original system and the upgraded system, HMIs were used. Furthermore, we did not know ‘normal’ intensity values, which would have been needed to choose the intensity for calibration sheet.

Table 4. Differences of measured intensities in two adapters in small LCDs.

Intensity LCD number	Adapter #1	Adapter #2	Original adapter
1	88	91	141
2	96	fail	140
3	94	92	140
4	89	88	134
5	80	78	127
6	83	83	135
7	85	84	135
8	85	84	128
9	86	87	133
10	88	85	136

Table 5. Differences of measured intensities in two adapters in large LCDs.

Intensity LCD number	Adapter #1	Adapter #2	Original adapter
1	126	124	155
2	123	122	155
3	116	114	146
4	127	124	157
5	121	119	151
6	130	129	160
7	121	119	152
8	122	121	153
9	123	121	153
10	122	120	153

6. DISCUSSION AND DEVELOPMENT IDEAS

In the previous chapters, we presented the current test system and evaluation of the system. The current system is now giving promising results, but more improvements can be done. In this chapter, we are discussing findings, development of the system, further development ideas, and limitations. Some ideas were not possible to put into action during the time frame as the changes need more testing and can not be implemented straight to the production testing.

6.1 Development of the fail detection

Upgraded adapters were adapted into production after brief testing in the maintenance site. Production test results were monitored to get information about function of the current system and to react as fast as possible to the possible errors.

In both LCD sizes, can be seen changes in the LCD test fault amounts. Previously, the LCD test has given most of all faults (Figure 21). Test results for large LCD are shown in Table 6 and for small LCD are shown in Table 7. These results are from two-month period, both from the original system before the improvement has started, and from the current, improved, system. Comparison of the results is better seen in Figure 31 and 33, in which the original system results are normalized to be comparable with the current system results.

With the current system, 142 large LCD faults were detected within 3856 tested products, when 169 faults were detected within 5460 tested products with the original system. The original system has less large LCD faults than the current system, but the increase can be explained by other reasons. During this work, faults in vlcd test has increased. Vlcd test measures voltage of the LCD. We have noticed that contrast of an LCD affects to a value of the vlcd test. Higher value in vlcd test can be linked to higher contrast, which can be seen as a drop of intensity of the LCD (Figure 32). However, all LCDs with high vlcd value do not fail in the intensity test because the backlight of the LCD can be brighter

depending on the product batch. Although, in LCDs with high voltage intensity is notable lower than in LCDs with lower voltage. All LCDs with high intensity values have also lower vlcd value. The current system finds well the LCDs with low intensity LCDs, when the original system let them pass the test. In practice, the original system was having larger tolerance compared to the current system.

Table 6. Production test results of large LCD before and after HMI test adapter upgrade.

Tests	Original system	Amount (%)	Current system	Amount (%)
Number of tested products	5460		3856	
Failed products	643	11,78	534	13,85
LCD test	169	3,10	142	3,68
vlcd test	95	1,74	141	3,66
Ethernet connector test	97	1,78	100	2,59
Indicator LED test	117	2,14	35	0,91
Regulator test	23	0,42	4	0,10
Write product information	9	0,16	35	0,91
Firmware upload	81	1,48	35	0,91
Other	79	1,45	39	1,01

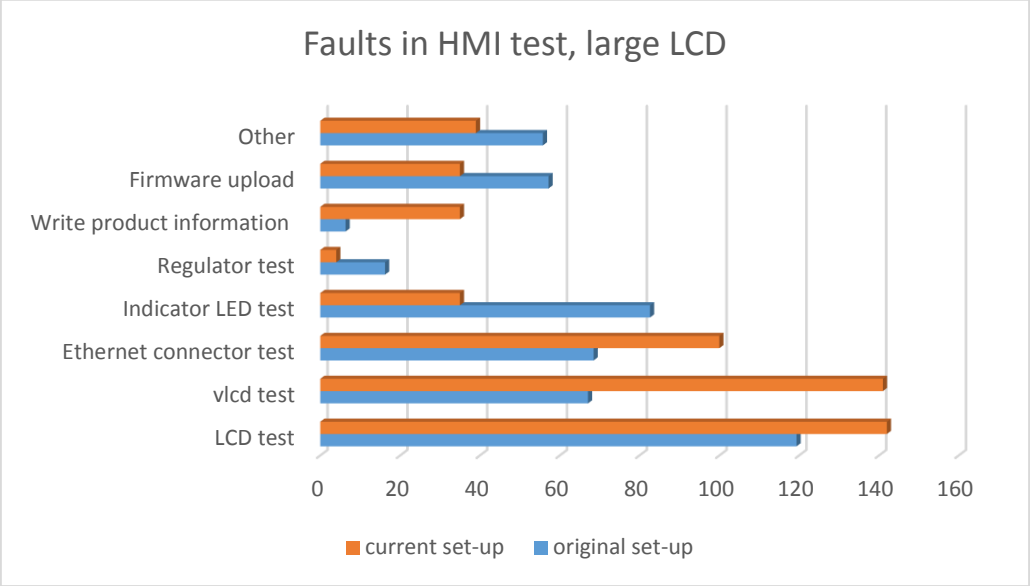

Figure 31. HMI with large LCD test comparison between the original and the current set-ups. Blue is the original set-up and orange is the current set-up.

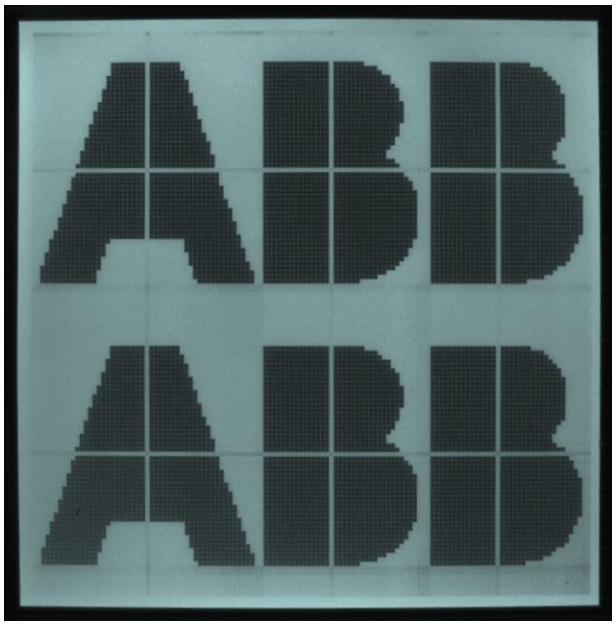

Figure 32. Effect of high contrast in large LCD with high vlcd measurement. High vlcd is noticed to be linked up with high contrast and thus, low intensity. Also, reflections of the pixels can be noticed.

The amount of faults in small LCD is decreased compared to the original system. The original system gave 129 LCD test fails with 3028 tested products, and the current system 24 LCD test fails with 1676 tested products. This shows that number of failed products have decreased significantly.

Image distortions have been problematic in small LCD test, which can be seen in fault amounts. Distorted image will fail both in pixel detection and bitmap comparison, and the fault can be only 1 to 2 pixels. With the changes in the system we could improve the accuracy of the testing and reduce negative faults significantly. There is still the problem with the intensity of the backlight LEDs of the small LCD, which needs more investigation and improvements. In addition, tightening of intensity tolerances need to be thought.

Table 7. Production test results of small LCD before and after HMI test adapter upgrade.

Tests	Original system	Amount (%)	Current system	Amount (%)
Number of tested products	3028		1676	
Failed products	402	13,28	138	8,23
LCD test	129	4,26	24	1,43
Ethernet connector test	47	1,55	57	3,40
Indicator LED test	34	1,12	10	0,60
Firmware upload	35	1,16	15	0,89
Write product information	5	0,17	7	0,42
Regulator test	89	2,94	2	0,12
Other	63	2,08	23	1,37

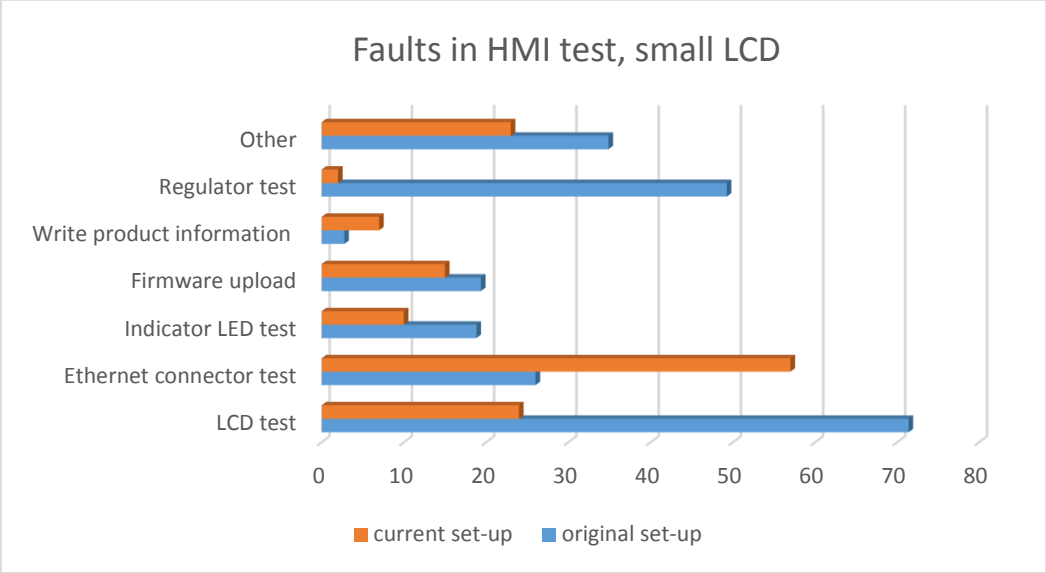

Figure 33. HMI with small LCD test comparison between the original and the current set-ups. Blue is the original set-up and orange is the current set-up.

Because of decreased amount of LCD faults, other faults will pop up and they can be taken under investigation. Fault types such as ‘ethernet connector test’ and ‘regulator test’ have increased. This may be because of the adapter, station on a module. For example, if contact between module and adapter is not good enough, these tests can fail. Especially regulator test faults could be caused by detrition of adapter needles. This is only speculation as more investigation is needed.

6.2 Spatial calibration

In the original system, the old calibration image captured with the first ever set-up was used. New grid image for calibration was taken for the current system. For accuracy, a grid image should be taken with the same camera and the same FOV as test images. The significance of the right calibration is high because all lens and cameras cause different distortions.

Another option for the grid image is a chequered grid image (Figure 34). The chequered image has more clear straight lines than the dot image. The software may have easier to process the calibration with existing lines than the lines that are created according to the dots. The chequered image includes more reference points over the image than the dot grid image. Every line can be thought as reference. Moreover, intersections of lines can be detected more accurately compared to the interpolated lines in the dot image. Altogether, overall interpolation and verification of the calibration may be easier with the chequered image. To improve system more, the chequered image should be considered, which requires changes in software.

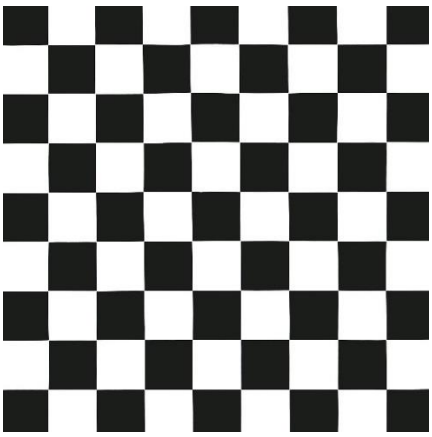

Figure 34. Chequered calibration grid image.

6.3 Camera and lens

As was mentioned previously, camera properties and optics meets the requirements set. Optimal optics would be a camera and lens with longer focal length, for instance 16mm to 25mm, which would give the accuracy of one pixel, that not possible with the current set-up. Longer focal length needs also much longer working distance, such as several tens of centimetres. In our set-up, the working distance is short, just ten centimetres, which is possible only with short focal length. Short focal length gives wider angle of view

compared to longer focal length, but longer one gives higher magnification. (Hecht 1987, Jan Kamp 2013)

Aperture was set to the aperture stop about f/3, which was mentioned to be the optimal aperture of the lens system This cut the brightness of captured images, as a smaller aperture reduces light, and thus the intensity of the image. Smaller aperture will cause deeper DOF than the larger aperture, which is useful in this test system as the small and the large LCD are in different distances from the HMI surface. At the current system, both LCD sizes can be focused at the same time. Furthermore, larger aperture gives brighter image, but it also causes an uneven intensity over the captured image, so called vignetting. (Hecht 1987)

6.4 Software

The software of this system has been developed about ten years ago, and it would need more improvements that can be done during the thesis. Many industrial software providers (Section 3.6) offer the ready-to-use applications with wide scale of machine vision operations.

Machine vision operations of software of test system are limited and they fulfil the requirements stated in test specification, of which main points are listed in section 4.2.1. It has been developed to measure intensity and defect pixels. ROI defining algorithm is bearable, but more precise operations could be used. For instance, edge detection could be method to think of. The LCD of the HMI has straight edges and it is located at the constant position, which makes edge detection reasonable easy to implement, and for example, LabVIEW includes basic tools for edge detection. However, creating image processing operations for needs such as in LCD test, takes time and needs verification. Some machine vision software use real image templates, which are real images from a target, not bitmap images.

When considering a system to be used, it would be worth to try another company, which have more machine vision operations and which can be chosen and used by a customer. Then, it could be possible to use various machine vision operations.

The problem with small LCD displays have been the LED lights at the bottom of the display. Illumination of the display is uneven, when the bottom area of the display is lit up and the top of the display stays darker. This contrast difference caused plenty of HMI fails previously. However, changes in the aperture, exposure time and calibration have increased the camera seen illumination uniformity over the LCD surface. One method to consider is high dynamic range (HDR) imaging, which is used to create greater dynamic range over the image. This is done by taking various images from the same target with different exposure and then merging them to one image, in which luminance over the image should be increased. The method could help in the problem of small LCDs, in which intensity varies over the LCD surface.

During the tests, we noticed that the current system (neither the original system) could not detect scratches in the LCD surface. Detection of scratches would need different lighting, for example light from the side of the target. The side light causes reflection from the scratches, which could be detected. However, LCD surfaces should be inspected by the LCD manufacturer.

6.5 Light emitted diode analysis

LED analysis uses optical fibres to carry the intensity and colour information to the analysator. This process and LEDs itself have many challenges, which influence the quality of the analysis. The issues include the design of LEDs, variety of the membrane and LEDs position, and an attachment process of the LEDs. Moreover, the optic fibres and calibration of the LED analyser have issues that affect to the test result.

Electronics of the LEDs and schematic how they are set in the circuit have a strong effect to the intensity differences in the assembled product. The LEDs are connected in a group of three parallel LEDs, so current divides between those. Then one LED is brighter when lighting alone than when all three are on.

There are several membranes glued on top of each other. Positions of the membrane layers and the LEDs may vary, which can cause diffraction of the LED light and detection of dimmer intensity. LEDs are positioned on the sheet and supported with glue to avoid bending and position changes. The glue may change the intensity and wavelength of the LED light. In addition, every LED production branch have different illumination properties. Usually, difference may not be remarkable.

One possibility to measure LEDs in a more modern way is to use a camera and machine vision operations. This measurement style would remove the problems that optic fibres cause.

6.6 Test adapter

Test adapter includes various moving element that can cause problems during tests. For example, top of the adapter, push buttons and measurement needles. Problems can be avoided by accurate use of the adapter and regular maintenance. Next, we discuss about problems we faced during the work.

Test adapter should not let ambient light inside the adapter, and the only light source should be the display itself. Very bright LCDs create reflections inside the adapter that can be seen in test images. This can be avoided with antireflection coating, such as matt black painting. Moreover, reflections on the LCD surface can be seen if the cover of the camera is not positioned right, because the ambient light affects the measurement (Figure 35).

Some connection problems can be avoided by taking care of measurement needles and wires. Wearing out causes bad connection between part and a measurement point. Connection error like this can be, for example, Ethernet connection error when wire is in bad condition or voltage or reset tests that measured with needles in measurement plate.

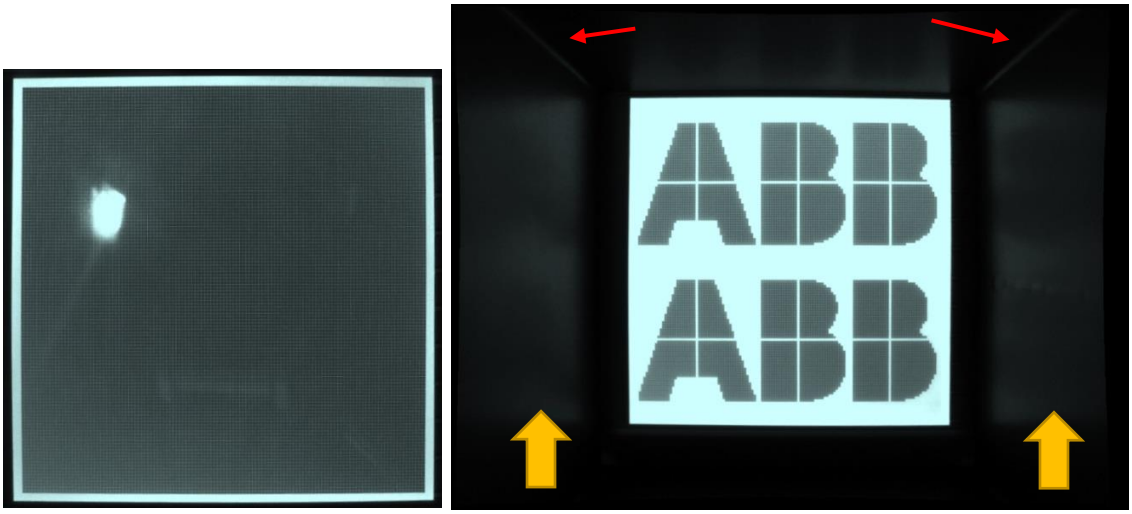

Figure 35. Left) Reflected light from outside the adapter causes bright spots in captured images. Right) Very bright LCDs cause reflections inside the adapter. Yellow arrows show reflection around the LCD and red arrows show reflections in corners.

6.7 Product series

The large and small LCDs are located differently on the surface membrane. This causes differences in working distances. The difference make camera positioning challenging, as there is no possibilities to change camera position between measurements. With the current system, both working distances are within the DOF of the camera, which means both of the LCD sizes can be in focus at the same time. That is good, as five camera adapters are located globally and no automatic moving system exists that could be used to change the camera position. Operators' work should include sources of errors as little as possible, so changing the camera position every time the LCD size changes, is not the option. Although, if focus seems to be problem in the future, automatic focus can be

thought. Investing to an automatic focus could provide accuracy of one pixel, but would also mean change of the system and higher costs of the lens.

On the top of the HMI is protection membrane, that should be removed before the HMI test. Some operators leave the membrane on the top of the HMI, which may affect test results. The LCD test does not detect the membrane (Figure 36), but detection of air bubbles under the membrane have been reported. Membrane itself may weaken the accuracy of the image analysis, even though it is not detected. For further improvement, the system should be able to detect the membrane, or at least the air bubbles under it. To clear up an influence of the membrane, more analysis has to be done.

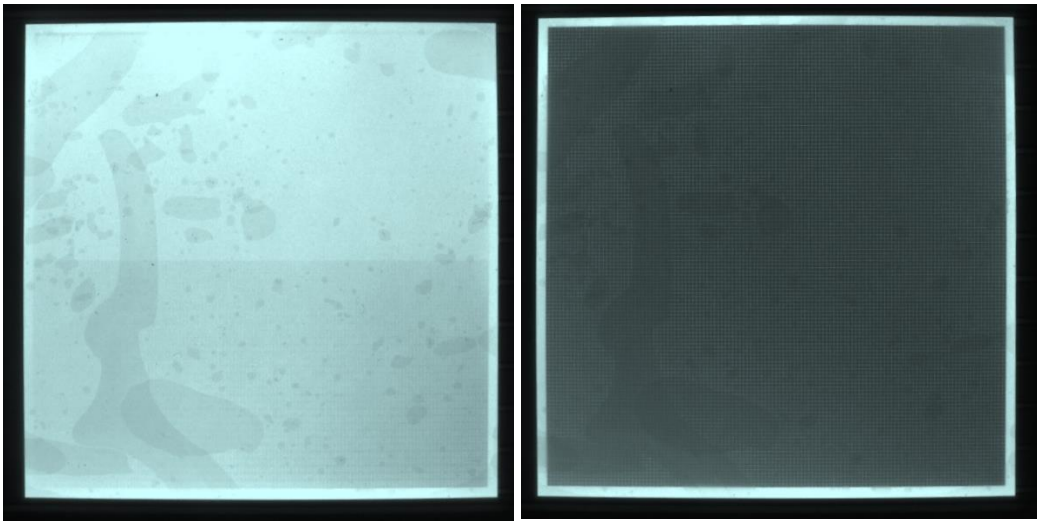

Figure 36. Protection membrane on top of the HMI can be seen in images captured during the LCD test. The membrane may affect the accuracy of the measurement.

Backlight LED intensity and LCD contrast vary between individual products. Variety causes challenges in the detecting of ROIs and pixels, and to defining tolerance values for the intensity. Example of intensity differences between products are illustrated in Figures 37. HMIs with small LCD have more problems with intensity differences because the small LCD has backlight LEDs, which intensity and place can vary depending on the production batch.

Figure 37. Differences between small LCDs intensities.

6.8 Limitations

The work included limitations, which were the illumination differences between products, differences in working distances, limited sampling set, production problems, increased occur of other HMI test faults and banned machine vision operation blocks. Partial solutions were found for all of these but still they affect the testing quality.

The software was partly from another company, and machine vision operations were done in banned blocks, which made understanding of the operations challenging. In the future, I suggest consideration of software, which has more finished layout or better support. At the moment, support is minimal.

System was developed to detect faults in two different size LCDs. In optimal situation, both of the LCD sizes has own adapter with proper settings. The LCDs are in different distances from the camera as the small LCD is lower than the large LCD. This may cause problems within the DOF. In the current system both LCDs are in usable focus because of aperture and camera settings.

Test sampling set was unnecessarily small as there were not opportunity to the large sampling set of HMIs. Larger verification of the test set-up modifications had to perform in PCBA-suppliers, which in fact gives more reliable results. However, detection and intensity measurement thresholds need more investigation before changes in production can be made.

7. CONCLUSION

The new camera and lens were installed into the HMI testing platform. The set-up and testing software were evaluated and tested to get a better idea about their functionality and possibilities. Various camera properties and software features were adjusted to improve the performance of the testing system. The camera set-up is now in better focus and system captures images with good quality in both LCD sizes. The understanding of the machine vision operations and camera settings of the system is better, and there is a guide for further use and adjusting.

The most important changes were the improvement of calibration and the changes in exposure settings. These changes decreased the number of negative faults of the small LCD significantly, which had positive effects to the FPY of HMIs. In addition, other faults in HMI tests can be taken under control as the LCD test is no longer the main fault type.

The pixel detection and intensity measurement accuracy were tested, and we noticed that the system could perform better by changing the tolerances. However, more data is required to make conclusions about tolerance changes. For intensity tolerance changes, the products should be inspected also with the naked eye to decide the limits for a ‘good’ intensity.

The system was noticed to be suitable only for the use it has been developed for, and in the future, new machine vision methods should be considered for ROI detection and template matching, or even using another industrial machine vision software company.

REFERENCES

ABB (2014), 630 Operational manual, Medium voltage products, ABB download centre.

ABB (2015), 620 Operational manual, Medium voltage products, ABB download centre.

ABB (2016), 615 Operational manual, Medium voltage products, ABB download centre.

ABB Distribution protection and control [Homepage], [Cited 15th Nov. 2016]. Available at: http://new.abb.com/medium-voltage/distribution-automation

Ahearn, Glen (2016), Know your needs for best machine vision camera selection, *Industrial Photonics*, 3:2, 13-15.

Bhardwaj, Saket & Ajay Mittal (2012), A survey on various edge detection techniques, *Procedia Technology*, 4 (2012) 220-226.

Chao, Shin-Min & Du-Ming Tsai (2007), An isotropic diffusion-based defect detection for low-contrast glass substrates, *Image and Vision Computing*, 26 (2008) 187-200.

Edmund optics (2011), Understanding Camera Sensors for Machine Vision Applications, [Homepage], [Cited 21st Oct. 2016]. Available at: http://www.edmundoptics.com/resources/application-notes/imaging/understanding-camera-sensors-for-machine-vision-applications/

Feasa (2013), [Homepage], [Cited 2nd Jan. 2017]. Available at: http://www.feasa.ie/

Fujitsu (2015), Fujitsu develops technology to automate construction of visual-inspections programs for production-lines [Cited 9th Dec. 2016]. Available at: http://www.fujitsu.com/global/about/resources/news/press-releases/2015/1118-02.html

GigE Vision standard (2016), AIA [Homepage], [Cited 21st Oct. 2016]. Available at: http://www.visiononline.org/vision-standards-details.cfm?type=5

Goodman, Douglas S. (2010), General principles of geometrical optics. In: *Handbook of Optics*, eBook, McGraw-Hill.

Guyton, A. C. and J. E. Hall (2010), *Textbook of Medical Physiology,* Saunders, 12th edition, Philadelphia, PA, USA.

Harris, Chris & Mike Stephens (1988), A combined corner and edge detector, Proceedings of the 4th Alvey Vision Conference, page 147-151.

Hecht, Eugene (1987), *Optics,* Addison-Wesley Publishing company, US.

Hitachi Joei Tech. Co., Ltd., LCD Panel Assembly [Homepage], [Cited 9th Dec. 2016]. Available at: http://www.hitachi-je.co.jp/english/product/lcd/lcd.html

Huang, Szu-Hao & Ying-Cheng Pan (2015), Automated visual inspection in the semiconductor industry: A survey, *Computers in Industry*, 66 (2015) 1-10.

Huang, Thomas S., George J. Yang &Gregory y. Tang (1979), A fast two-dimensional median filtering algorithm. *IEEE Transactions on Acoustic, Speech and Signal Processing*, 27(1): 13-18.

Imatest Sharpness [Homepage], [Cited 2nd Dec. 2016]. Available at: http://www.imatest.com/docs/sharpness/

ISO 12233 (2014), Photography - Electronic still picture imaging - Resolution and spatial frequency responses.

I.S.X. Corp [Homepage], [Cited 9th Dec. 2016]. Available at: http://www.isx.co.jp/en/product/inspection01.html

Jain, Ramesh, Rangachar Kasturi & Brian G. Schunck (1995), *Machine Vision*, McGraw-Hill, New York, NY, USA.

Jan Kamp, Haje (2013), Everything About Camera Lenses, Photocritic Photo School [Homepage], [Cited 11th Jan. 2017]. Available at: http://www.photocritic.org/articles/everything-about-camera-lenses

Jiang, B. C., C.-C. Wang & H.-C. Liu (2007), Liquid crystal display surface uniformity defect inspection using analysis of varience and exponentially weighted moving average techniques, *International Journal of Production Research*, 43:1, 67-80.

Keelan, B. W. (2002), *Handbook of Image Quality*, CRC Press, Boca Raton, US.

Keyence Corporate Overview [Homepage], [Cited 2nd Jan. 2017]. Available at: http://www.keyence.co.uk/about-us/corporate/index.jsp

KeyenceVision systems [Homepage], [Cited 2nd Jan. 2017]. Available at: http://www.keyence.co.uk/products/vision/vision-sys/index.jsp

Larsen, Ronald W. (2011), *LabVIEW for Engineers.* Pearson, Austin, TX, US.

Lenhardt, Karl (2006), Optical systems in machine vision. In: *Handbook of Machine Vision*. WILEY-VCH Verlag GmbH & Co. KGaA, Weinheim.

Lindeberg, Tony (1994), *Scale-Space Theory in Computer Vision*. Kluwer Dordrecht, The Netherlands.

Logic technologies, LCM Production Assembly [Homepage], [Cited 9th Dec. 2016]. Available at: https://logictechno.com/lcm-production/

Nagao, M. & T. A. Matsuyama (1980), *A Structural Analysis of Complex Aerial Photographs*. Plenum Press, New York.

National Instruments (2011), NI Vision 2011 for LabVIEW Help, Filters, [Homepage], [Cited 2nd Jan. 2017]. Available at: http://zone.ni.com/reference/en-XX/help/370281P-01/imaqvision/filters_pal/

National Instruments (2017), [Homepage], [Cited 2nd Jan. 2017]. Available at: LabVIEW http://finland.ni.com/labview

Nica Technologies Pte., Ltd., Automation and Visual inspection [Homepage], [Cited 9th Dec. 2016]. Available at: http://www.nicatech.com.sg/automation-visual-inspection/

OptoFidelity (2012), OptoFidelity DIT (Display Inspection tool), User Manual.

OptoFidelity (2013), DIT Display Inspection tool, Product datasheed, [Cited 27th Oct. 2016] Available at: http://www.optofidelity.com/files/uploads/2016/04/OF_DIT_En.pdf,

Optofidelity [Homepage], [Cited 27th Oct. 2016]. Available at:, http://www.optofidelity.com/optofidelity/

Orbis systems [Homepage], [Cited 7th Dec. 2016] Available at: http://www.orbissystems.eu/

Orbis systems Products [Homepage], [Cited 7th Dec. 2016] Available at: http://www.orbissystems.eu/en/products/

Park, No Kap & Suk In Yoo (2009), Evaluation of TFT-LCD defects based on human visual perception, *Displays* 30 (2009) 1–16.

Peltoketo, Veli-Tapani (2016). *Benchmarking of mobile phone cameras*, University of Vaasa 2016.

Radiant vision systems [Homepage], [Cited 7th Dec. 2016]. Available at: http://www.radiantvisionsystems.com/applications/display-test

Rahunen, Krista, Kimmo Kallio & Jarmo Alander: Testing of displays of protection and control relays with machine vision, Automaatiopäivät22 seminar, oral presentation, March 2017, Vaasa.

Sergiyenko, Oleg & Julio C. Rodriquez-Quinonez (2016), *Developing and Applying Optoelectronics in Machine Vision*, Hershey.

Siemens (2011), 7SG11 Argus 8, [Cited 9th Dec. 2016]. Available at: http://sm-industry.ru/titan_img/ecatalog/7SG118%20Argus%208%20Technical%20Manual%20Chapter%207%20Commissioning%20(R7).pdf

Siemens, Simatic Machine Vision, [Cited 7th Dec. 2016]. Available at: https://www.siemens.be/eit/microautomation/downloads/SIMATIC_VS110_EN.pdf

Sonka, Milan, Vaclav Hvalac & Roger Boyle (2008*), Image Processing, Analysis and Machine Vision*, Thomson, Toronto, Ontario.

Steger, Carsten (2008), Machine vision algorithms. In: *Handbook of Machine Vision*, WILEY-VCH Verlag GmbH & Co. KGaA, Weinheim, p. 511-692.

Takano Co., Ltd.Image Processing Group [Homepage], [Cited 7th Dec. 2016], Available at: https://www.takano-kensa.com/english/html/film/03_pattern.html

Telljohan, Axel (2006), Introduction to building a machine vision inspection. In: *Handbook of Machine Vision*, WILEY-VCH Verlag GmbH & Co. KGaA, Weinheim, p.35-72.

Tsai, Du-Ming & Shia-Chih Lai (2008), Defect detection in periodically patterned surfaces using independent component analysis, *Pattern Recognition*, 41, 2812-2832.

Tyan, S. G. (1981), Median filtering, deterministic properties. In: *Two-Dimensional Digital Signal Processing*. Springer Verlag, Berlin.

Van Droogenbroeck, Mark & Hugues Talbot (1996), Fast computation of morphological operations with arbitrary structuring elements. *Pattern Recognition Letters*, 17(14):1451-1460.

Wang, X. (2008), *Noise in Sub-Micron CMOS Image Sensors*. Enschede, Netherlands.

Watson, Andrew B. (2006), The spatial standard observer: A human vision model for display inspection, invited paper, *Society for Information Display Technical Digests*, 37 (2006) 1312-1315.

Wilson, Andrew (2013), Understanding distortion in machine vision, Vision Systems Design [Homepage], [Cited 11th Jan. 2017], Available at: http://www.vision-systems.com/articles/print/volume-18/issue-7/features/understanding-distortion-in-machine-vision-lenses.html

Winkler, Stefan (2013), Characteristic of human vision. In: *Perceptual Digital Imaging – Methods and Applications*, Taylor and Francis group, Boca Raton, FL, US.

Yole (2015), Status of the CMOS image sensor industry.

APPENDIX A.

Figure 1A-11A shows the tests with coffee grounds to determine threshold values for target detection.

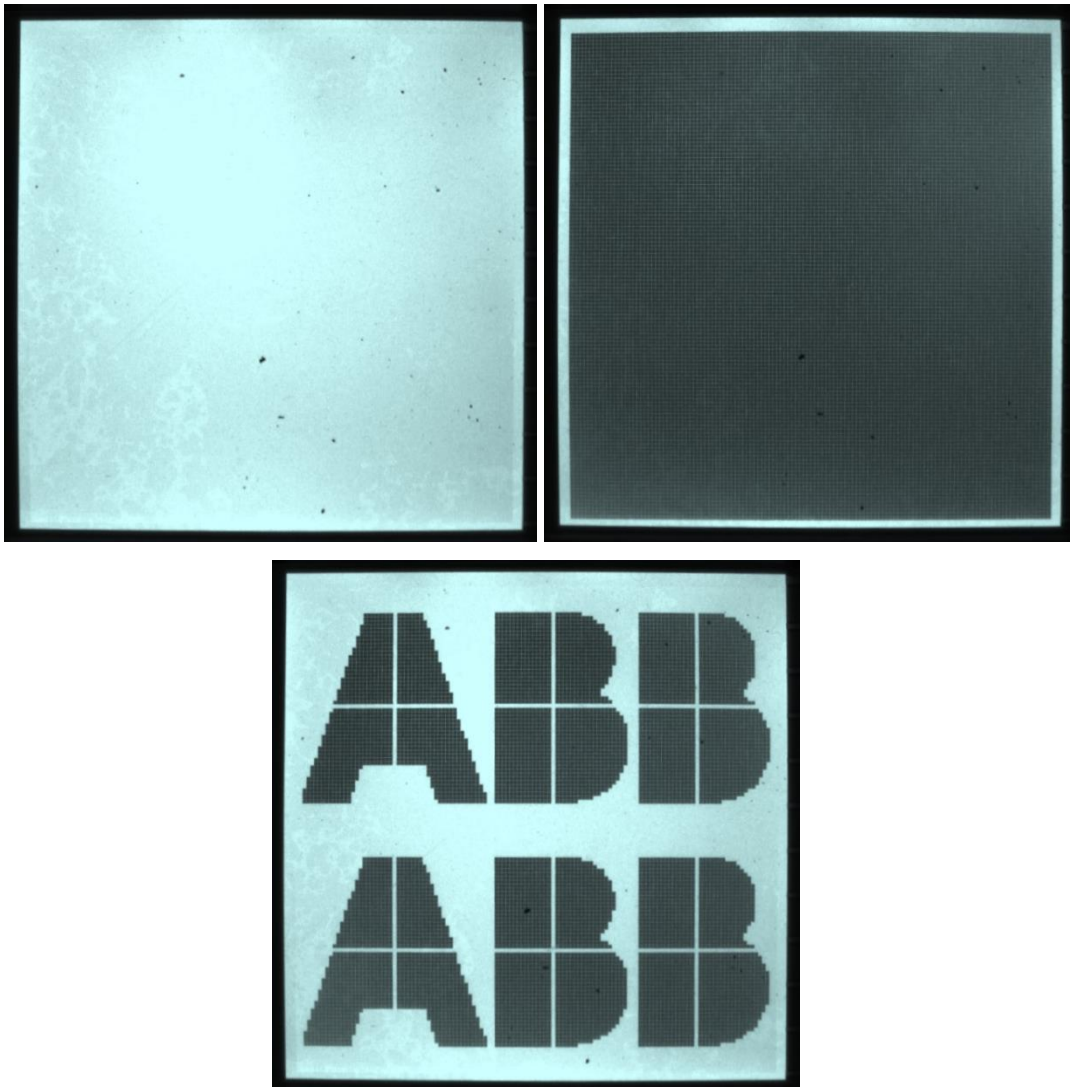

Figure 1A. Image of large LCD with current values: pixellimit_in 30 and pixellimit_out 15. The detection percent is always zero, which means that every detected fault is reported. The small black dots are coffee grounds to simulate pixel defects and trash on the LCD panel. Top left) all pixels off image. Top right) all pixels on image. Bottom) bitmap image.

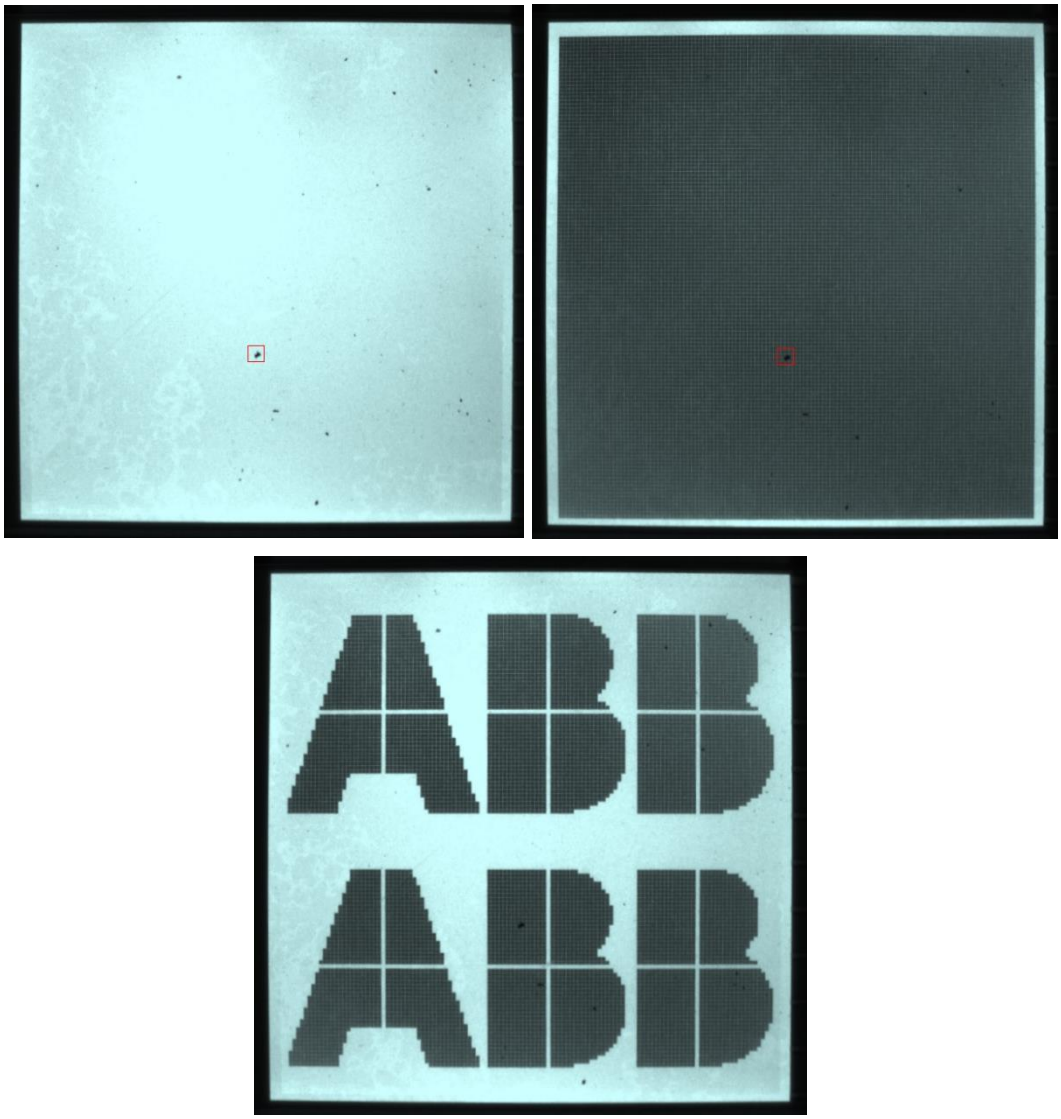

Figure 2A. Image of large LCD with values that can detect smaller pieces of coffee grounds. The grounds can be seen also in figure 1A, but because of threshold values, they are not detected. The values of pixellimit_in 90 and pixellimit_out 15 give the first images with detection of coffee grounds. Top left) all pixels off image. Top right) all pixels on image. Bottom) bitmap image.

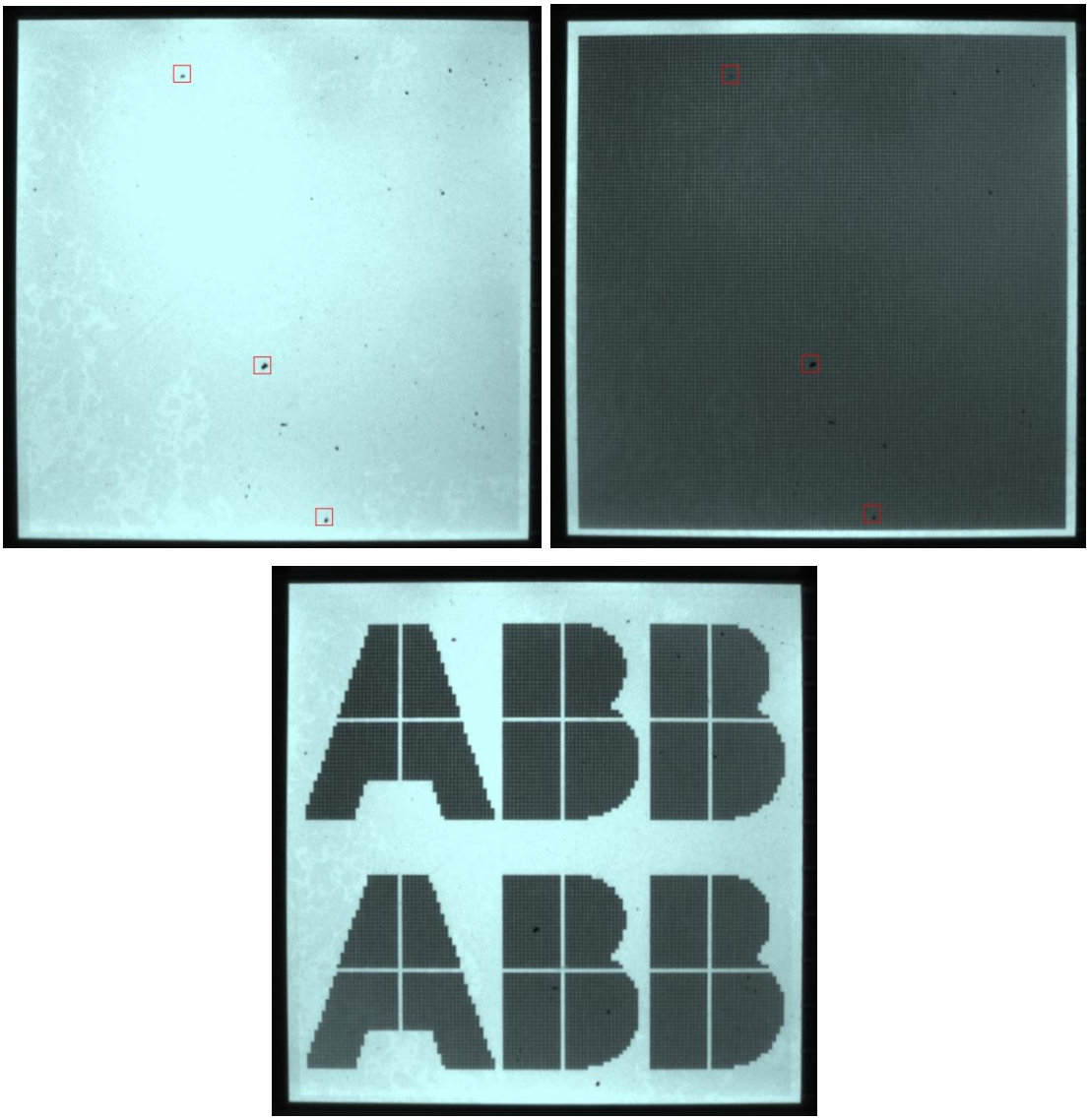

Figure 3A. Image of large LCD with values that can detect coffee ground more accurately. The values are: pixellimit_in 100 and pixellimit_out 15. With these values, smaller pieces can be detected than what is shown in figure 2A. Top left) all pixels off image. Top right) all pixels on image. Bottom) bitmap image.

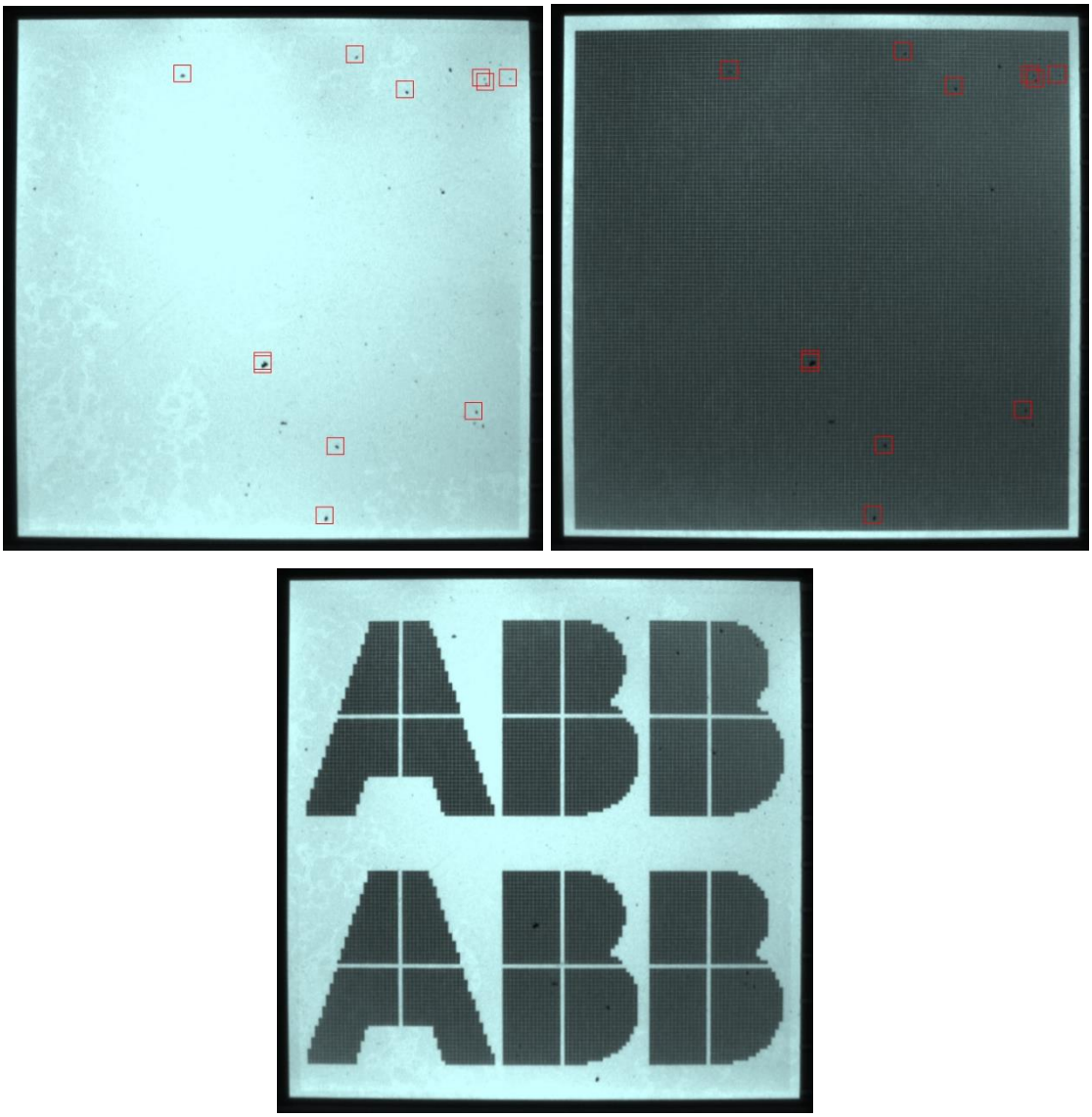

Figure 4A. Image of large LCD with values that can detect smaller coffee ground more accurately. The values are: pixellimit_in 120 and pixellimit_out 15. With these values, smaller pieces can be detected than what is shown in figure 2A. As the bitmap image is only compared to the bitmap template, the small coffee grounds do not cause faults in that. Top left) all pixels off image. Top right) all pixels on image. Bottom) bitmap image.

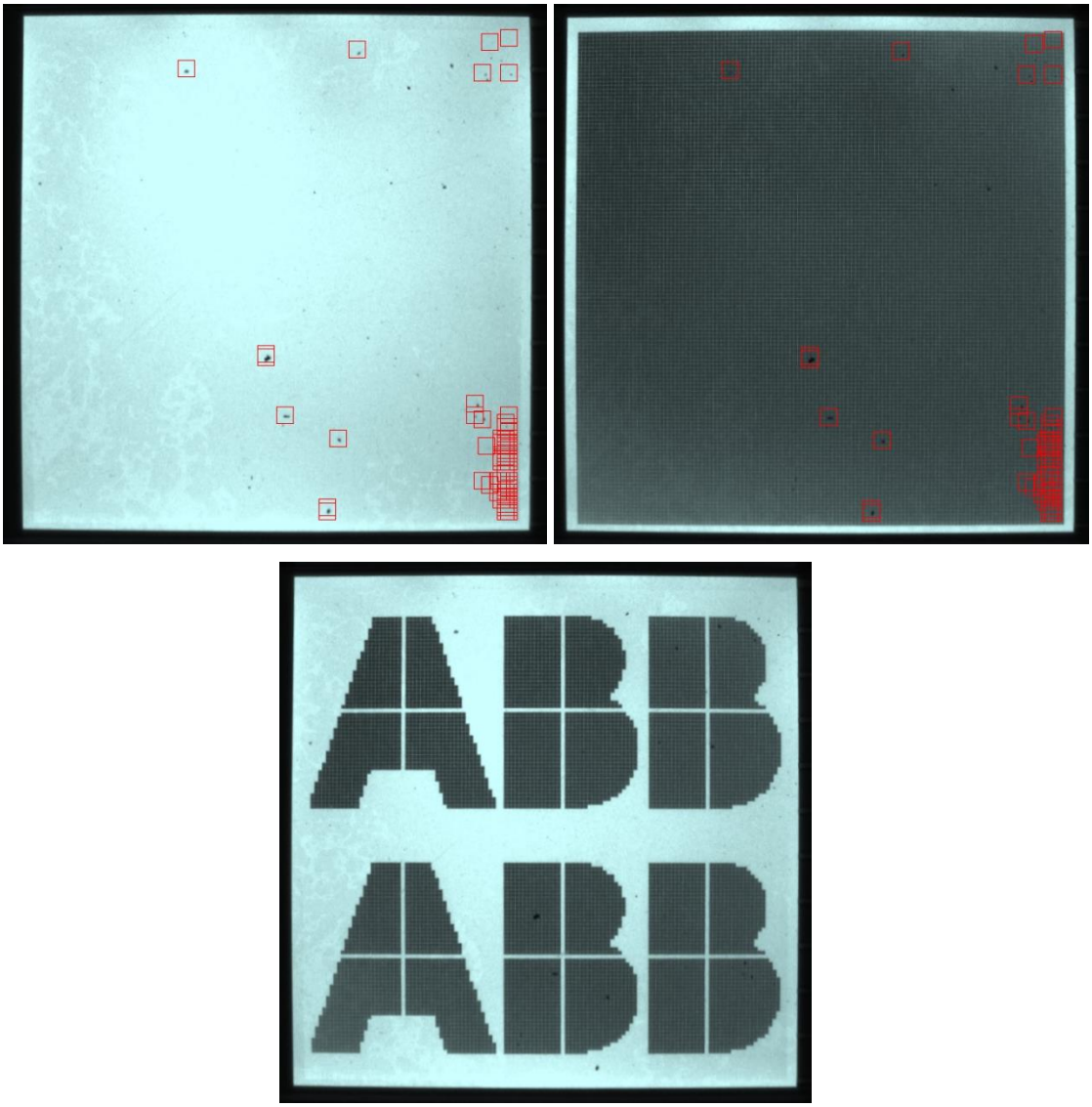

Figure 4A. Image of large LCD with values that can detect smaller coffee ground more accurately, but also edge pixels are detected. The values are: pixellimit_in 120 and pixellimit_out 80. With these values, smaller pieces can be detected than what is shown in figure 2A. Top left) all pixels off image. Top right) all pixels on image. Bottom) bitmap image.

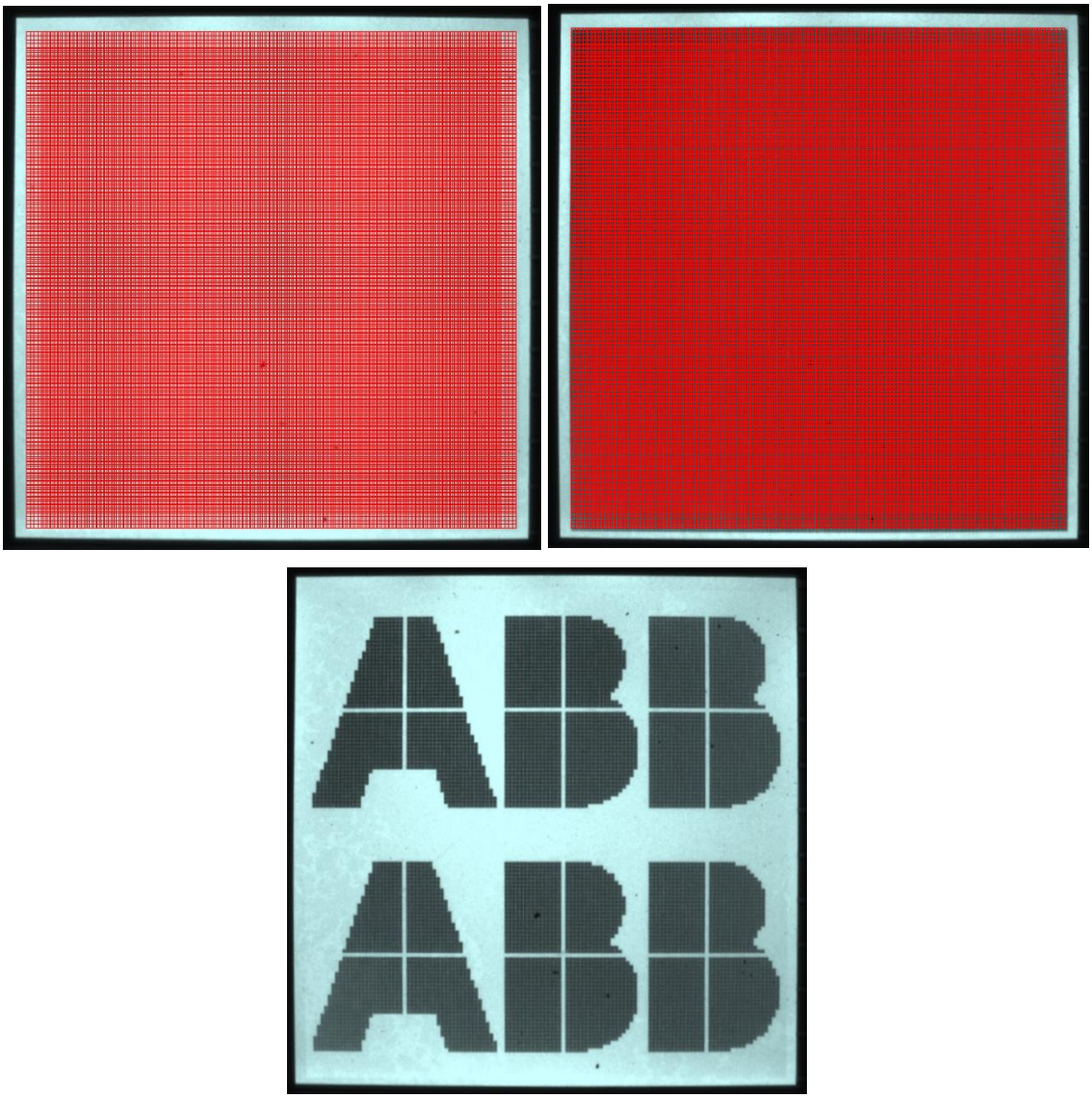

Figure 6A. Image of large LCD with fake faults. When the threshold is increased greatly, the fake faults appear. The threshold is too tight and does not give space to the natural intensity changes. The values are: pixellimit_in 200 and pixellimit_out 15. Top left) all pixels off image. Top right) all pixels on image. Bottom) bitmap image.

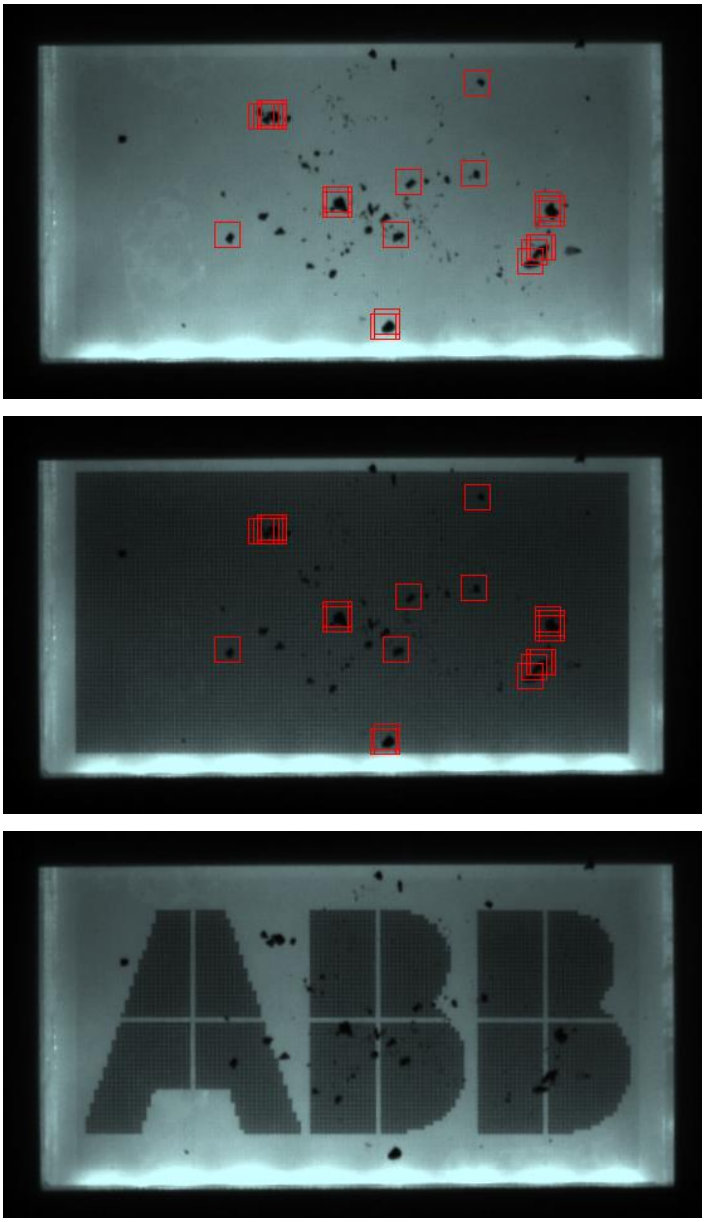

Figure 7A. Image of small LCD with current values: pixellimit_in 20 and pixellimit_out 5. The detection percent is always zero, which means that every detected fault is reported. The small black dots are coffee grounds to simulate pixel defects and trash on the LCD panel. This image includes large coffee grounds, which are detected. Although, in good test system, smaller parts should be detected. As the bitmap image is only compared to the bitmap template, the small coffee grounds do not cause faults in that. Top) all pixels off image. Middle) all pixels on image. Bottom) bitmap image.

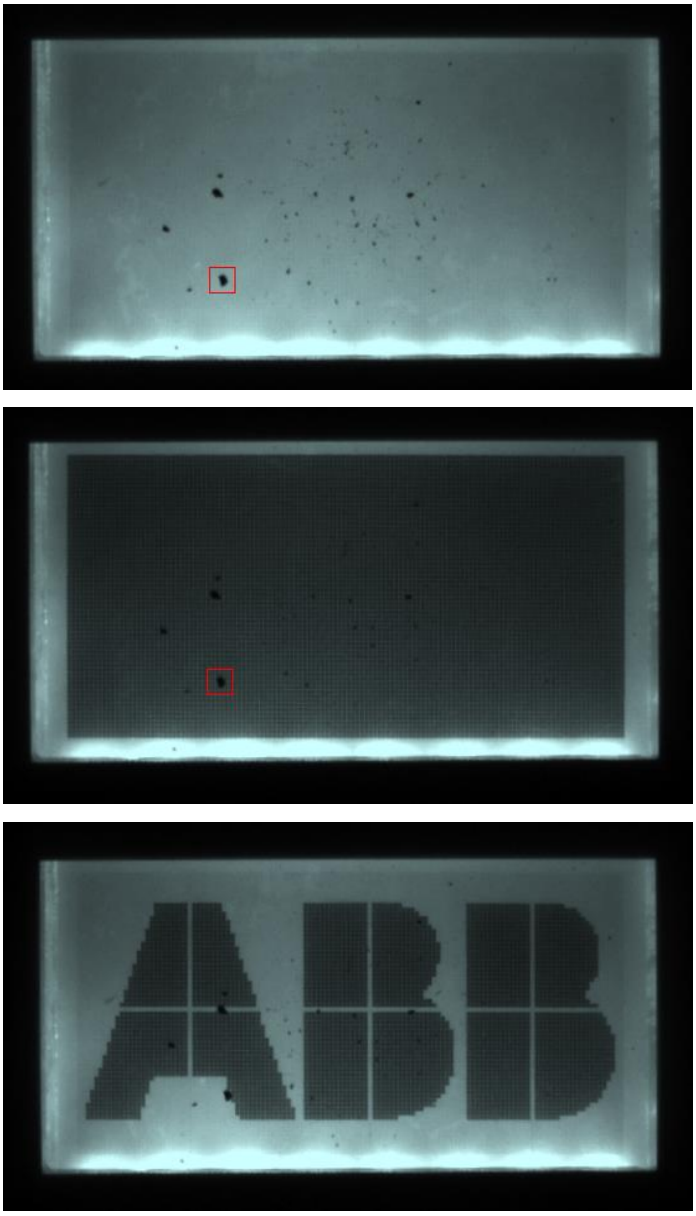

Figure 8A. Image of small LCD with current values: pixellimit_in 20 and pixellimit_out 5. The small black dots are coffee grounds to simulate pixel defects and trash on the LCD panel. This image includes smaller coffee grounds, and only one is detected. Although, in good test system, smaller parts should be detected. Top) all pixels off image. Middle) all pixels on image. Bottom) bitmap image.

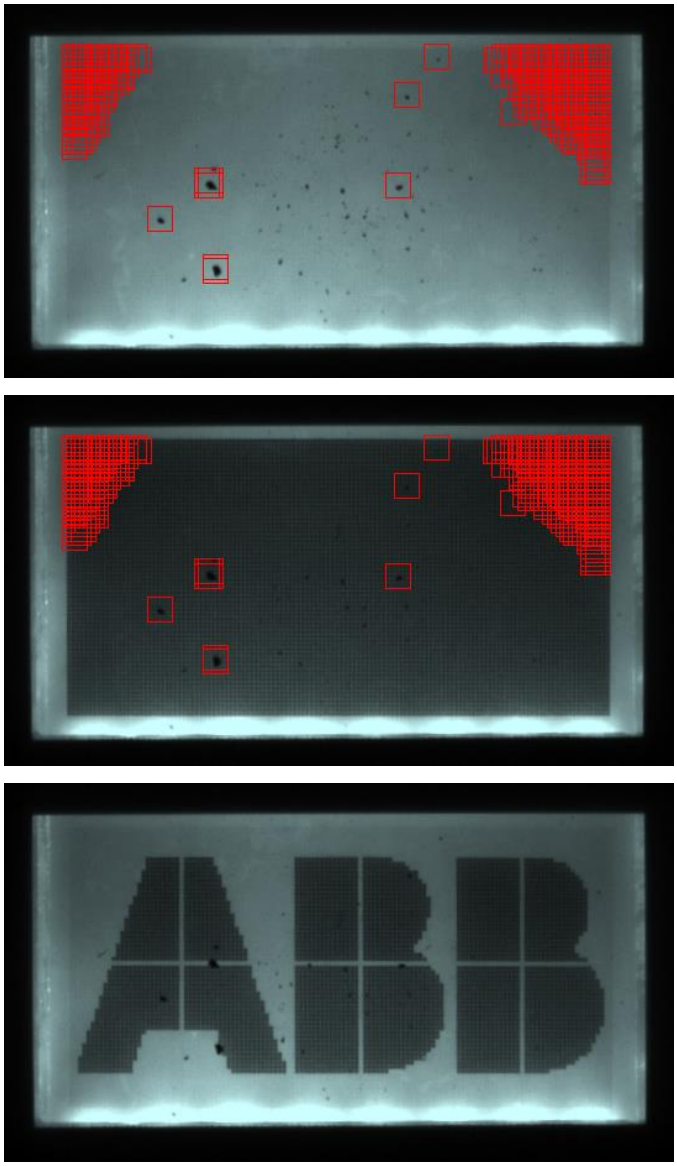

Figure 9A. Image of small LCD with current values: pixellimit_in 50 and pixellimit_out 5. This image includes smaller coffee grounds, and they are detected more accurately than in figure 7A. However, the application starts to detect false faults both in middle and edge area. The areas detected are the dimmer areas at the corners of the small LCD, where the natural variance of pixel intensity is smaller than in other area (better lighting). Top) all pixels off image. Middle) all pixels on image. Bottom) bitmap image.

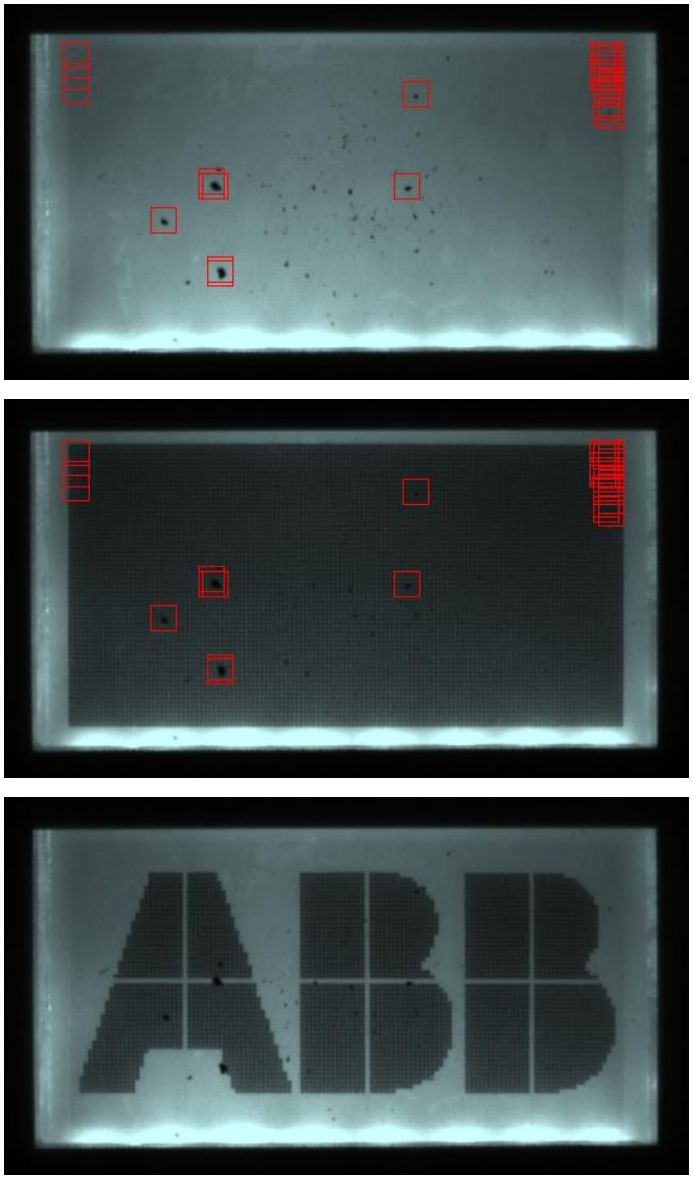

Figure 10A. Image of small LCD with current values: pixellimit_in 40 and pixellimit_out 15. Top) all pixels off image. Middle) all pixels on image. Bottom) bitmap image.

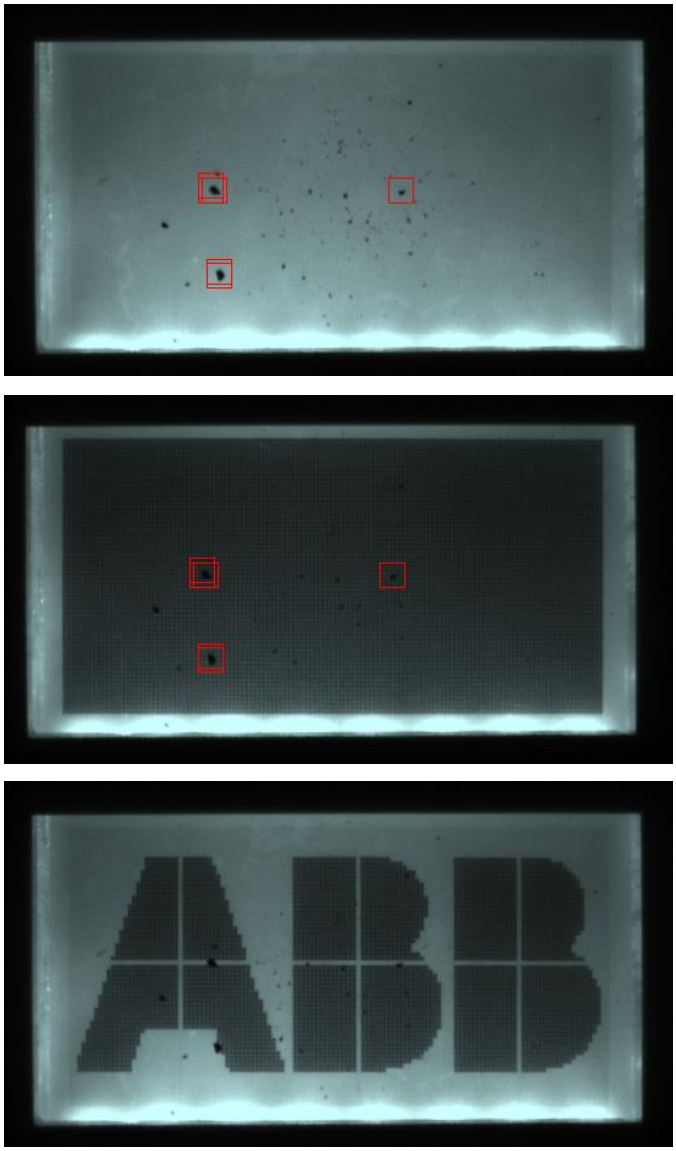

Figure 11A. Image of small LCD with current values: pixellimit_in 35 and pixellimit_out 10. Top) all pixels off image. Middle) all pixels on image. Bottom) bitmap image.

APPENDIX B.

Effect of the change in aperture size. Small aperture was size f/4, normal aperture f/3, and large aperture f/1.8.

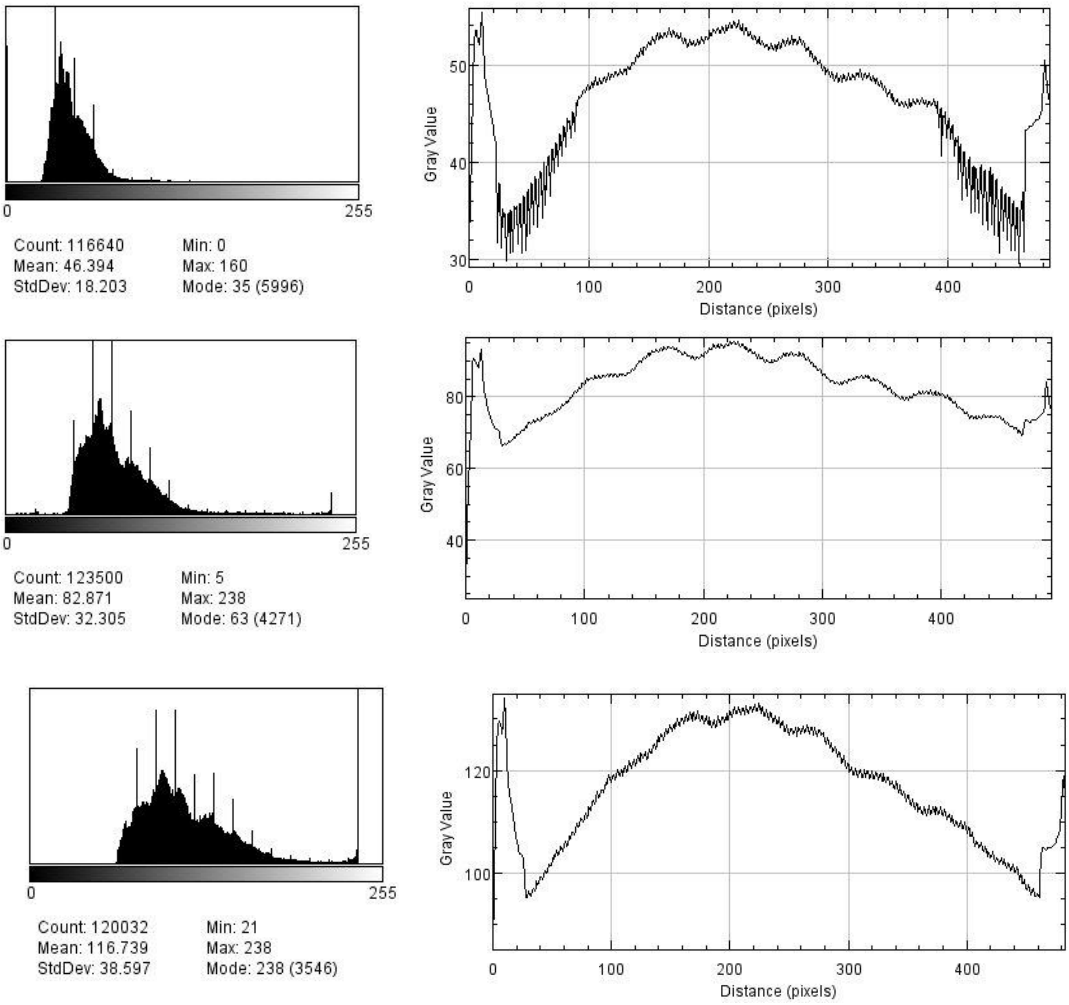

Figure B1. Histograms and plots of the images of small LCD. Top) small, Middle) normal, Bottom) large aperture size.

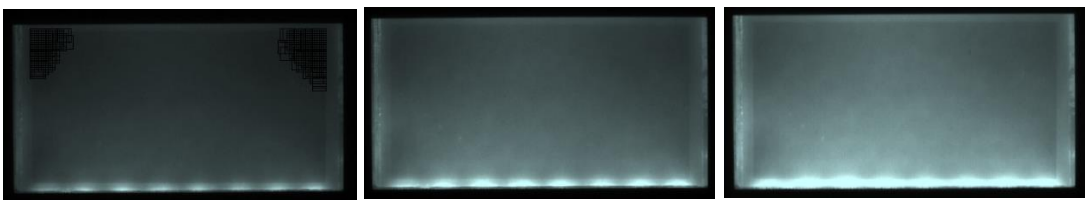

Figure B2. Small LCD captured with different aperture sizes: f/4, f/3 and f/1.8 respectively.

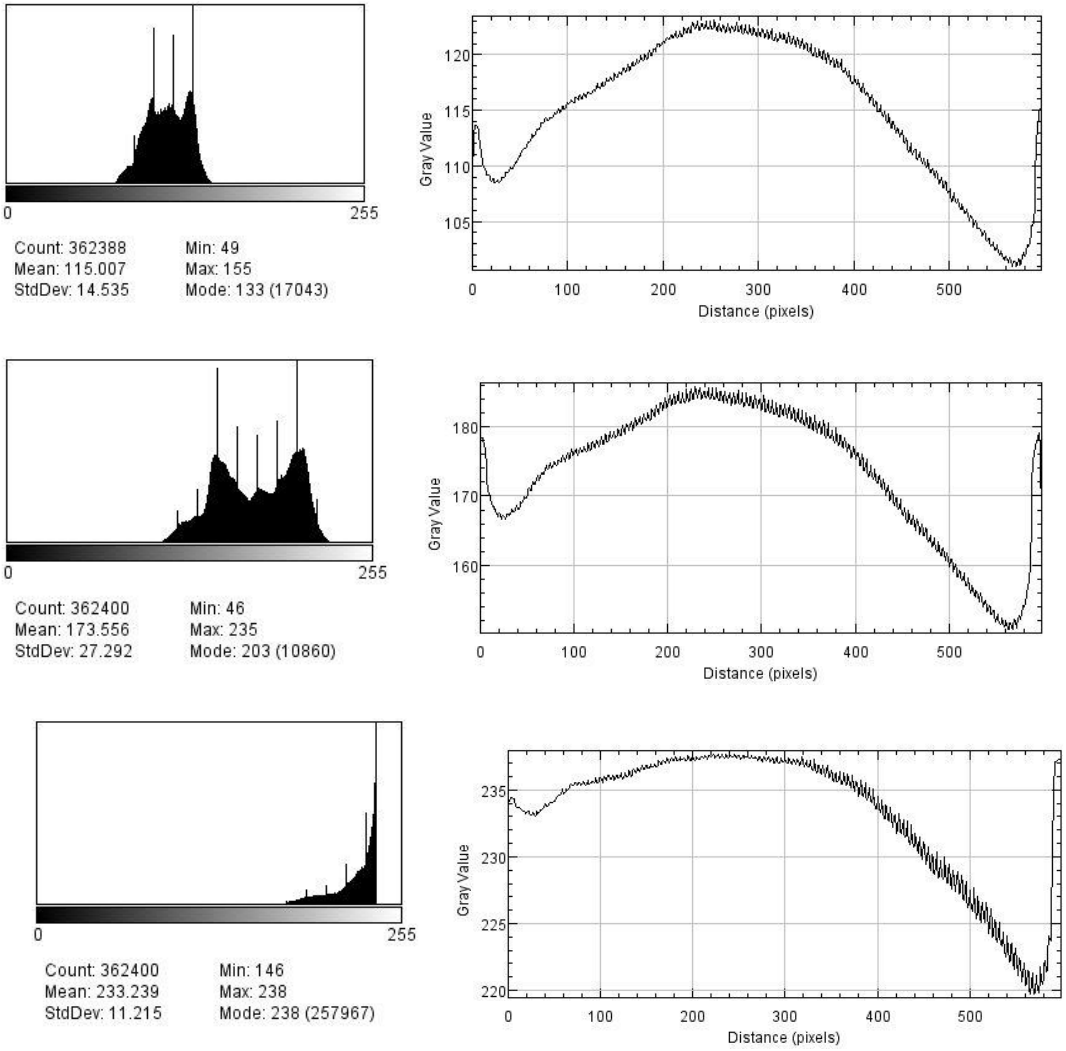

Figure B3. Histograms and plots of the images of large LCD. Top) small, Middle) normal, Bottom) large aperture size.

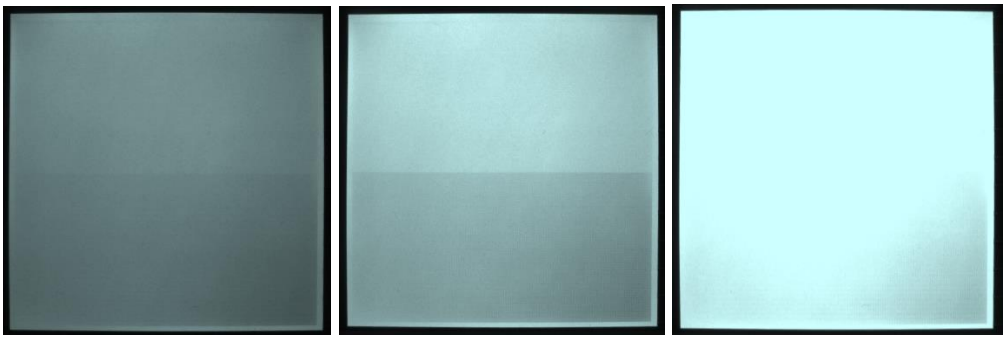

Figure B4. Large LCD captured with different aperture sizes: f/4, f/3 and f/1.8 respectively.

BACKGROUND MATERIAL

Appendices C.-F. are hidden due to Non-Disclosure Agreement.